DEVELOPMENT OF A THREE-AXIS LONG-PERIOD SEISMOGRAPH

Ivan Simon

Little (Arthur D.), Incorporated
Cambridge, Massachusetts

16 February 1970

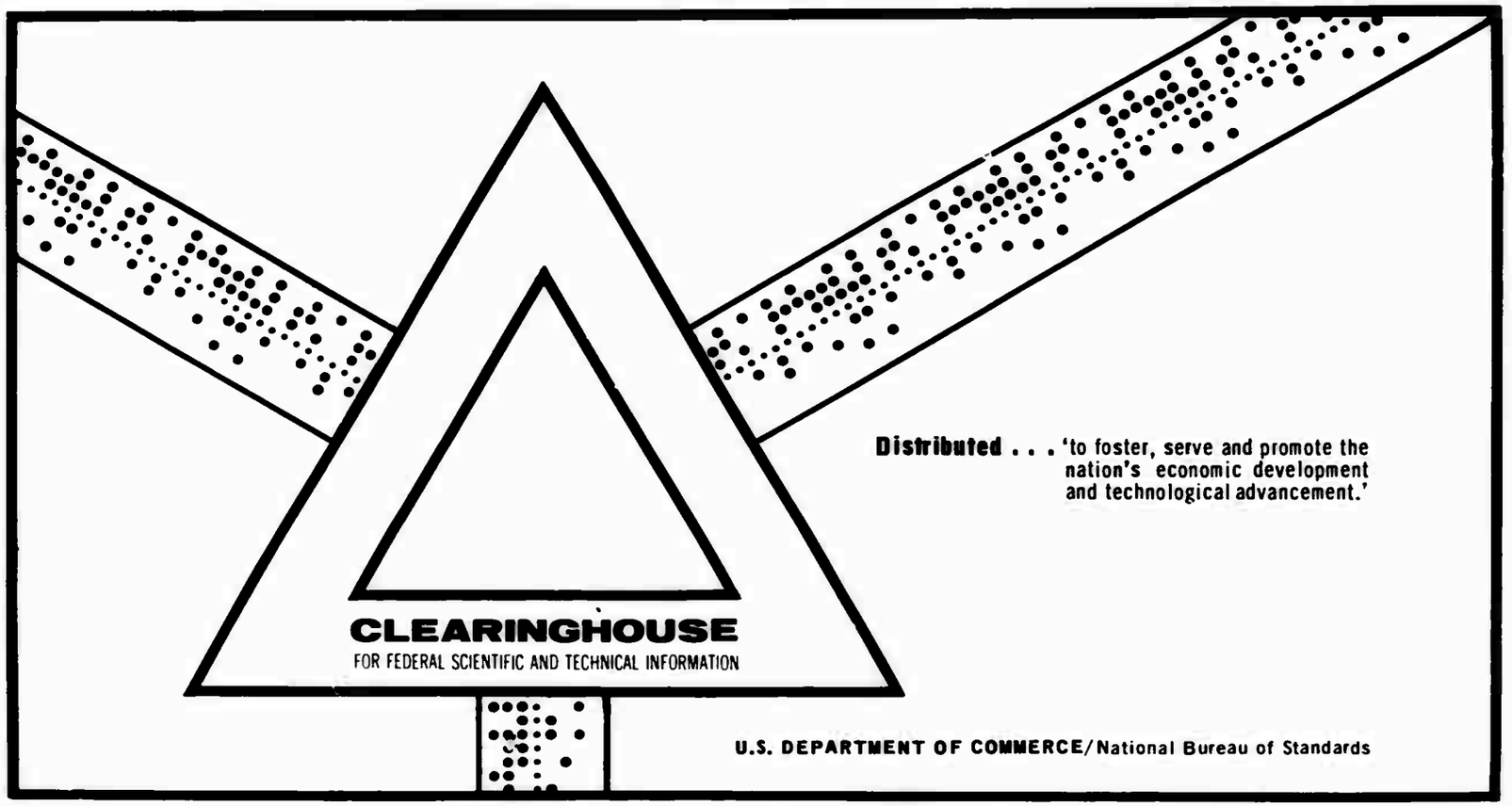

AFOSR 70-0526 TR

DEVELOPMENT OF A THREE-AXIS LONG-PERIOD SEISMOGRAPH

Final Report

prepared for

AIR FORCE OFFICE OF SCIENTIFIC RESEARCH
ARLINGTON, VIRGINIA

Arthur D. Little, Inc.

82

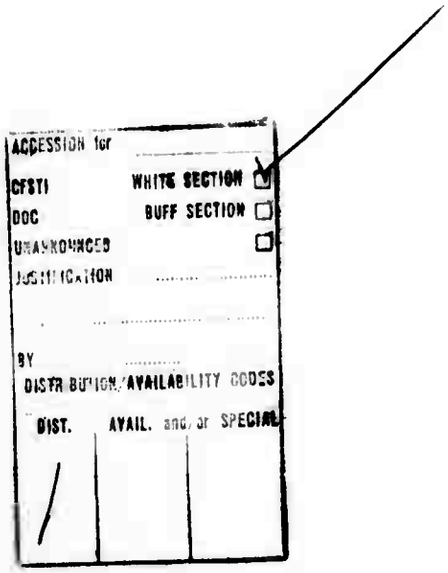
ACCESSION for
CFSTI WHITE SECTION
DDC BUFF SECTION
UNANNOUNCED
JUSTIFICATION
BY
DISTRIBUTION/AVAILABILITY CODES
DIST. AVAIL. and/or SPECIAL

FINAL REPORT

1 June 1967 through 31 December 1969

DEVELOPMENT OF A THREE-AXIS LONG-PERIOD SEISMOGRAPH

Sponsored by

Advanced Research Projects Agency
Nuclear Test Detection Office
ARPA Order No. 1029
Program Code No. 7F10

C-69429

Arthur D Little, Inc.

IDENTIFICATION

Project Title:	Development of a Three-Axis Long-Period Seismograph
ARPA Order No.:	1029
ARPA Program Code No.:	7F10
Name of Contractor:	Arthur D. Little, Inc.
Date of Contract:	1 June 1967
Amount of Contract:	$244,450
Amount of Amendment P001:	$208,995
Amount of Amendment P002:	$ (1,201)
Amount of Amendment P004:	$ 34,223
Total:	$486,467
Contract No.:	F44620-67-C-0107
Project Scientist:	Ivan Simon
Telephone Number:	(617) 864-5770

TABLE OF CONTENTS

LIST OF FIGURES

LIST OF FIGURES (Continued)

LIST OF FIGURES (Continued)

ABSTRACT

A three-axis, long-period, compact seismometer system utilizing a feedback-controlled seismic transducer based on a novel magnetic suspension principle was developed, constructed and tested. The system includes digital tape recording and data processing. The overall system response is flat (to 3db) over a pass band from 0.02 to .07 Hz and the dynamic range is 60 db. Results of tests show that surface waves from teleseismic events of $m_b \leq 5$ are consistently recorded. Horizontal components of surface waves from earthquakes of $m_b \geq 4.2$ in the Gulf of California region have been observed at the Ogdensburg, New Jersey test site.

I. INTRODUCTION

1 SEISMOLOGICAL BACKGROUND

This report describes the development of a new type of three-axis long-period seismometer system suitable for operation in boreholes of small (6 in. I.D.) diameter. At the time of the initiation of this work it was anticipated that large aperture seismic arrays will be equipped with high-performance, long-period seismographs and that such instruments will be placed in deep boreholes similar to those used for emplacement of the short-period seismographs in the LASA. In view of a great number of holes to be drilled for this purpose and because of the steep rise of cost with increasing diameter of borehole it appeared to be economically desirable to keep the size of the instruments as small as practical.

The general reasons underlying these plans derived from the existing need for improvement in the capability for discrimination between earthquakes and explosions of small magnitude recorded at teleseismic distances. The methods for solution of this problem have been under constant development during the past decade and became so effective that it is now possible to make a positive identification of any event as an earthquake or an explosion provided its magnitude is greater than $m_b = 4.75$[(1)]. The capability for discrimination requires a combination of criteria, among which the long-period contents of the received signal and the depth of the source are the most important.

Recording of long-period waves is essential because earthquakes and explosions differ significantly in the proportion in which the wave energy is partitioned between the short-period and long-period regions of the seismic spectrum. This observation is the basis of the so-called AR criterion[(2)] which requires determination of the area of the envelope of a long-period seismogram

containing most of the surface wave phases of the recorded event. A refinement of this criterion makes use of the separated Rayleigh or Love phases in a fashion similar to the AR method.

While separation of these two types of waves is possible, in principle, by their polarization it is found in practice to be far more difficult to obtain consistently good L-phase records than those of the R-phase. The reason for it is that horizontal seismographs are much more affected by spurious instabilities of the site than the vertical seismographs. When operated in shallow vaults long-period horizontal seismometers are limited in their useful magnification by the high level of ground noise resulting mostly from atmospheric pressure fluctuations. It is a common occurrence that they are out of operation for extended periods of time as a result of surface tilts caused by environmental effects. For this reason long-period horizontal seismometers should be located on stable, underground rock formations or in deep boreholes. High-performance, long-period seismometers utilizing pendulous transducers sealed in pressure-tight tanks[3] are not suited for installation in boreholes because of their large size.

Development of the magnetic suspension and its subsequent applications in tiltmeters[4] led us to propose its use in long-period seismometers of small physical size. Practical feasibility of such instruments was demonstrated during the first year of the project and a number of horizontal (six) and vertical (three) seismometers were subsequently built and tested. Even though it was not expected that instruments of this type would exceed the performance of the existing high-gain long-period seismometers, we found in final tests that the performance of the best of our horizontal instruments was comparable to that of the advanced station-type instruments such as described in reference[3]. Performance of our vertical seismometers was found to be less satisfactory because of high internal noise.

Maximum useful magnification of any seismograph is limited by the amount of noise generated internally (Johnson noise and Brownian motion) and externally (microseisms) within the limits of the signal pass band. If the internal noise of the seismometer were negligible the smallest detectable seismic signal would be limited only by the prevailing level of the microseismic noise. This noise varies considerably with the location of the site, geology of the area and weather conditions. The frequency distribution of the microseismic noise likewise varies with these factors, in particular in the long-period region. Nevertheless the general shape of the power spectrum of microseisms is fairly well established and may be exemplified by Figure 1, based on Haubrich and McCamy's analysis of the low-frequency microseismic noise at the center point of LASA[5]. The minimum of the microseismic noise is found, typically, around 0.03 Hz (33 sec. period) and the minimum power density, in terms of mean square displacement per unit bandwidth may be as low as 10^{-9} cm^2/Hz. Under adverse conditions the microseismic noise may increase by two orders of magnitude or more. The noise level rises rapidly on either side of the minimum. On the low frequency side the noise is largely of a local (non-propagating) origin resulting from fluctuations in barometric pressure loading, wind, etc. On the high frequency side the noise rises to the well known peaks at 0.075 and 0.15 Hz resulting from the propagating modes of coastal and pelagic origin.

The signals being sought are primarily surface waves of the Love and Rayleigh types generated by teleseismic events. Because of the velocity characteristics of the earth's crust and upper mantle surface, waves from teleseismic events are highly dispersed and form wave trains of many minutes duration whose energy is concentrated predominantly in a frequency band between approximately 0.025 and 0.10 Hz (10 to 40 sec.). Below 0.01 Hz, the energy of the signal becomes insignificant except for the largest natural earthquakes.

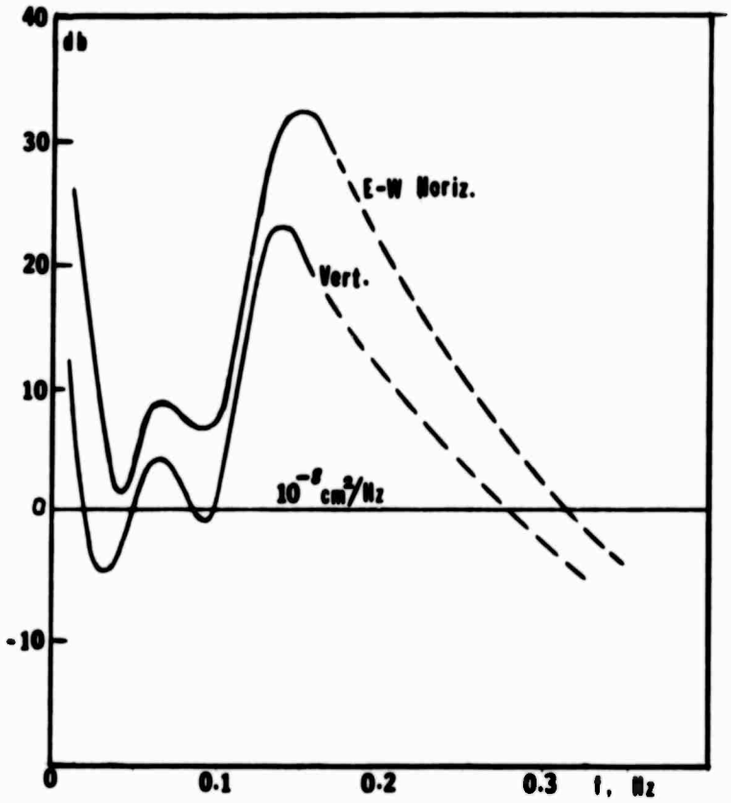

FIGURE 1 RELATIVE POWER SPECTRUM OF MICROSEISMS RECORDED BY THE LONG-PERIOD SEISMOMETERS AT THE CENTER OF LASA (After Haubrich and McCamy, 1967)

2. SYSTEM DESIGN CONSIDERATIONS

In view of the above considerations we concluded that the center frequency of a long-period seismometer system intended for detection of surface waves from small events at teleseismic distances should be around 0.03 Hz and the response of the system should drop off rapidly (at least 12 db/octave) below 0.02 and above 0.04 Hz. The frequency response curve of the system eventually adopted in our work is shown in Figure 2. The seismometers used in the system had frequency response essentially flat (in terms of acceleration) from 0 to approximately 0.5 Hz by virtue of the feedback control. The system response curve (in terms of displacement) of Figure 2 was obtained by a combination of active filters.

Feedback control was adopted early in the developement of the magnetic suspension seismometers for the following reasons:

a. Feedback control makes it possible to operate the seismic transducer in grossly underdamped state which aids to minimize the Brownian noise otherwise enhanced by the use of small seismic mass. The necessary damping is provided in the feedback loop.

b. The effective spring constant of the seismic mass can be adjusted at will and thus the response of the seismometer can be extended over a wide frequency range.

c. The performance of the feedback seismometer is insensitive to any possible changes in the physical characteristics of the magnetic suspension. This is helpful in duplicating the exact frequency response characteristics from one instrument to another.

d. The linearity of the feedback seismometer using a displacement readout sensor is improved and its dynamic range increased.

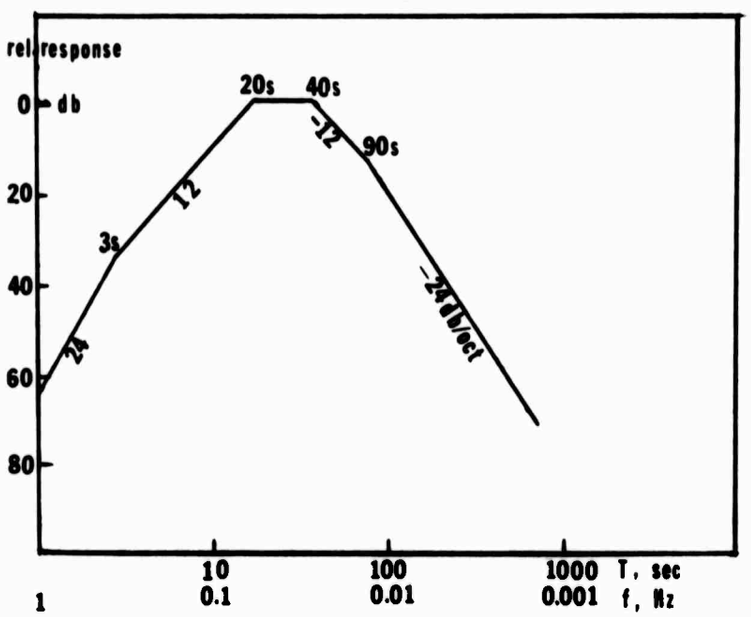

FIGURE 2 FREQUENCY RESPONSE CURVE OF THE ADL SEISMOMETER SYSTEM (Asymptotic Representation)

Application of feedback control requires use of a forcer acting upon the seismic mass in a strictly linear fashion over the expected range of displacements and frequencies. In order to preserve the desirable properties of the magnetic suspension no wires, springs, etc. must be attached to the seismic mass; hence, only field type forcers can be used. In the horizontal seismometer we used piezoelectric transducers to control the tilt of the base of the instrument and thus to exert a force proportional to the applied control voltage. In the vertical seismometer a magnetic field forcer was used to deliver a force proportional to the control current passing through a pair of gradient coils surrounding the suspended bar magnet.

In contradistinction to the classical seismometers which use a velocity sensing readout we adopted a displacement sensing readout for the seismometers of the magnetic suspension type. The quantity sensed is the displacement of the seismic mass relative to the frame of the seismometer. Conversion of displacement to voltage is obtained by means of a differential photocell of the photoresistive (CdS) type. Photoelectric readout of this type requires no bodily contact with the seismic mass and hence is preferable with diamagnetic suspension for the reasons given above. Moreover, unlike capacitive or inductive displacement readouts, it exerts no force on the seismic mass in the direction of sensitive axis. Some of the CdS photocells used in the readout proved to generate excessive noise at low frequencies. Silicon cells of equivalent size and electrical characteristics became available only late in the course of the project and could not be tested in the completed seismometers. All seismometers were to be built as self-contained units of identical shape and size (cylinders 4.75 in. O.D., 11 to 13 in. long) so that they could be stacked by three in a borehole package provided with a hole-lock.

From the outset of the project we decided that the output data of the complete system would be recorded digitally by an incremental, multi-channel magnetic tape recorder. Computer programs were developed for reading the tapes and to perform various computational operations on the data as required for visual presentation, digital filtering, noise analysis, zero crossings analysis, etc. Graphical recording by means of conventional pen-and-chart recorders was used only for monitoring of a few system channels in order to facilitate the selection of time intervals containing events of particular interest. This proved to be a good arrangement as it provided both instantaneous, visible information at all times and possibility for subsequent signal processing and detailed analysis when desired. Visual presentation of final results was made by computer plots on time and amplitude scales selected for best resolution of the detail of interest. In this way magnification could be adjusted over a wide range.

II. DESCRIPTION OF SEISMOMETERS

1. HORIZONTAL SEISMOMETERS

The principle of operation and the theory of the horizontal seismometer using the diamagnetic suspension were discussed in detail in our preceding annual report[6]. For reasons of completeness we shall only briefly outline in the following the present embodiment of the seismometer itself and its electronic feedback control circuitry. The construction of the horizontal seismometer is shown schematically in Figure 3 and in a photo, Figure 4. In Figure 3, M represents the magnet system used to levitate the seismic mass m, RL is the remote leveling unit and PZT is the piezoelectric forcer used for feedback control of the displacement of the seismic mass.

The seismic mass is a graphite rod 2.5 in. long, 0.086 in. in diameter, and approximately 0.80 gm in weight. It is levitated by a strong, inhomogeneous field in a straight-edge-and-groove gap of the magnet assembly M. In the axial direction it is constrained by the slight increase of the field toward the front and back edges of the magnet assembly. The axial restoring force resulting from this effect tends to return the seismic mass to the central position with a free period of, typically, 15 sec. Deviation of the seismic mass from the central position is measured by the photoelectric displacement sensor containing a miniature long-life lamp L and a dual photocell PD of the CdS photoresistive type. When the seismic mass is in its central position a "flag" F attached to one of its ends casts a shadow bisecting exactly the two halves of the photocell. In the actual instrument both the lamp and the front face of the photocell are provided with glass light pipes which permit sharper separation of the two light beams and allow more compact placement of the components. The transfer constant of the optical readout is approximately 20 volt/cm.

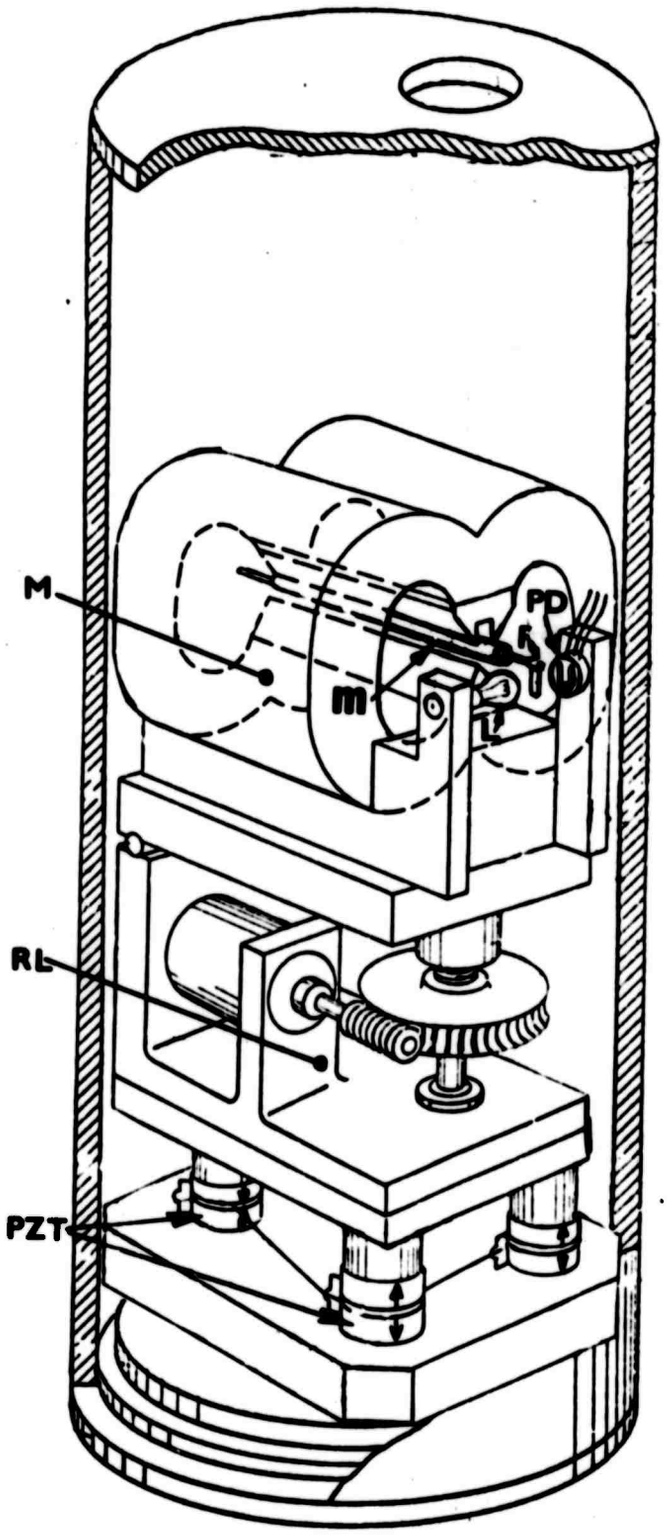

FIGURE 3 CUTAWAY VIEW OF THE HORIZONTAL SEISMOMETER
(Schematic)

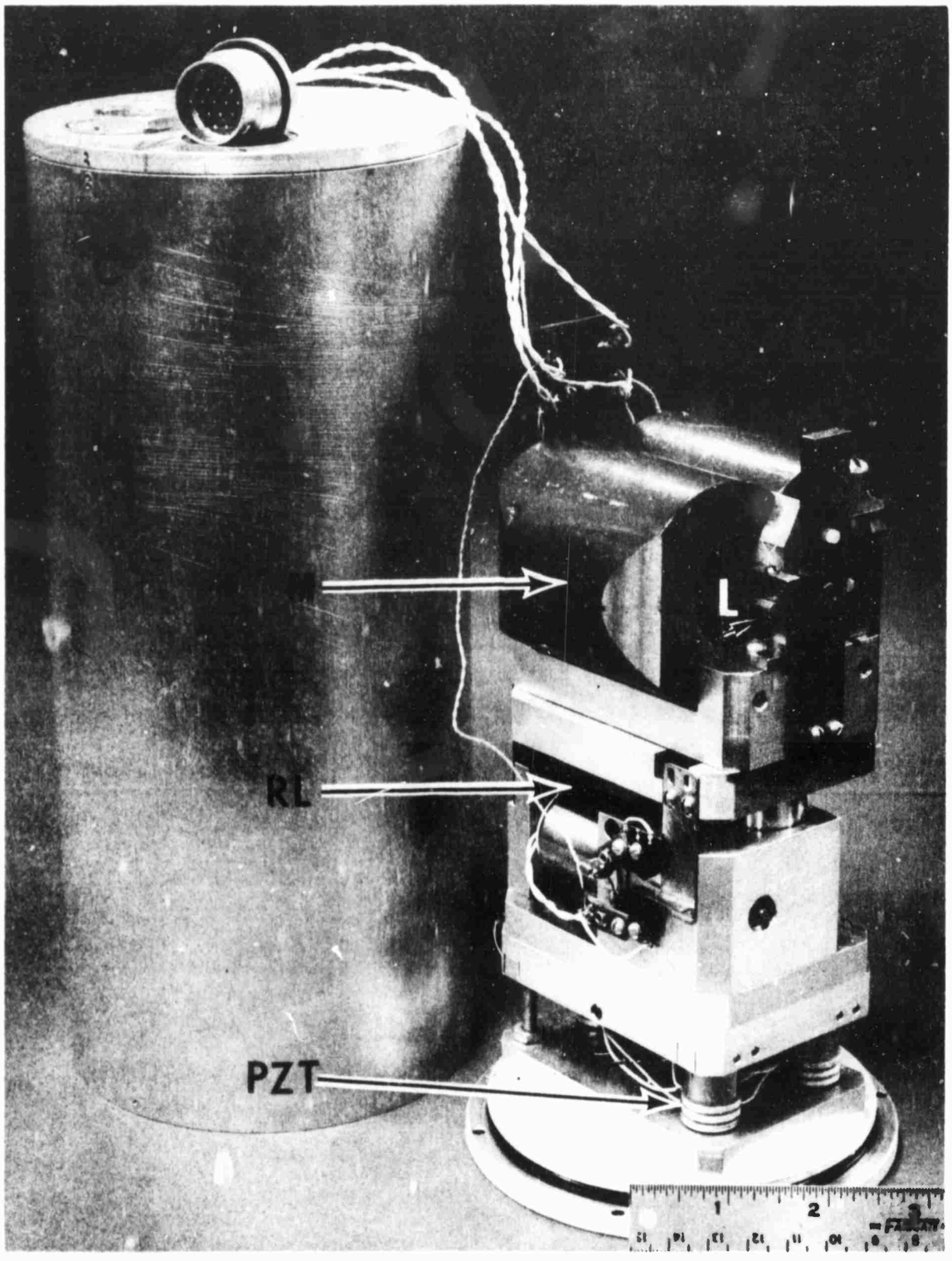

FIGURE 4 VIEW OF THE HORIZONTAL SEISMOMETER
(Photograph)

The seismic mass is freely suspended about its central position only as long as the entire assembly M is exactly horizontal. Leveling of the seismometer assembly is accomplished by the unit RL containing a motor-operated precision jack screw which has a range of $\pm 2^\circ$ of tilt and can be operated from the control panel either manually, or automatically. In the automatic mode of operation the unbalance current from the optical displacement sensor activates a bipolar relay which drives the motor in the direction necessary to restore the balance. Maximum movement of the seismic mass is limited by adjustable end stops (visible in Figure 4). Once the seismometer is emplaced and settled the remote leveling unit needs to be used only rarely, possibly to correct for varying level of the site, changes in temperature, etc. The degree of level unbalance is shown at all times by a meter L (Figure 5) located on the control panel.

Instantaneous displacements of the mass m relative to the frame caused by seismic movement of the ground are continually nullified by the electronic feedback control. The control force acting against the inertial force is obtained by tilting the base of the seismometer by applying voltage to stacks of piezoelectric ceramic discs PZT causing them to expand and contract as indicated by arrows in Figure 3. The piezoelectric coefficient of the material of discs, their thickness and the length of base give a forcer constant of approximately 5×10^{-5} cm/sec^2 per volt.

The feedback control circuit is shown in Figure 5. Amplifiers A_1, A_2 and A_3 are solid-state operational amplifiers; A_3 is a voltage amplifier required to raise the control voltage to the level (up to 100 volts) adequate for operation of the piezoelectric crystals. The frequency dependence of gain and phase necessary for obtaining proper forcing and damping of the underdamped ($\delta \approx 0.1$) seismic mass is accomplished by the network coupling the amplifiers A_1 and A_2. The gain and frequency of the gain step

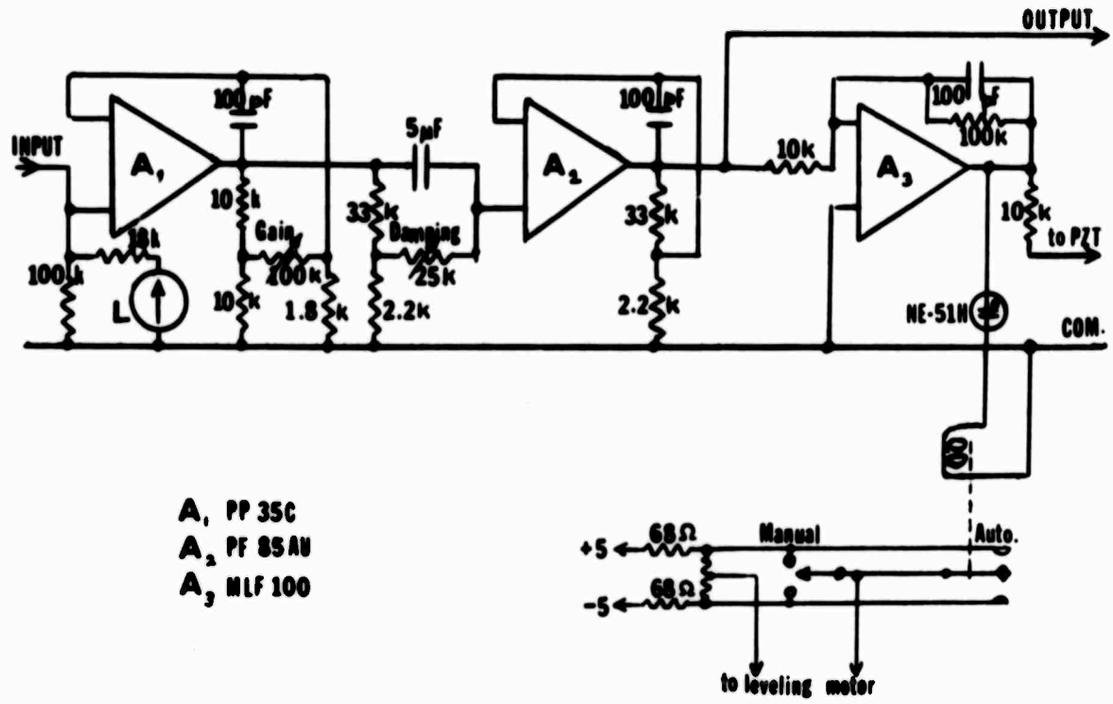

FIGURE 5 FEEDBACK CONTROL CIRCUIT OF THE HORIZONTAL SEISMOMETER

are adjustable over a wide range. Typical settings with a gain step of 1:16, allowing for a 4:1 gain variation over the operating frequency band, result in a voltage transfer function (including amplifier A_3) of the form (approximately) $10^4 \times (s+2)/(s+20)$. With the loop closed the seismometer is approximately optimally damped (≈ 0.7); typically, it has a responsivity to acceleration of 2000 to 4000 volts per cm sec^{-2}.

A later version of horizontal seismometer was constructed which used magnetic forcing in the feedback loop in place of the piezoelectric forcer system. The basic design of the instrument was the same as that described above, with the exception that magnetic coils were fitted to the ends of the polepieces as shown in Figure 6 and the piezoelectric forcer assembly was removed. Arrows show the direction of magnetic field imposed by current in the four coils. Instead of exerting a restoring force upon the seismic mass by tilting the seismometer, restoration was achieved by altering the magnetic field strength at the ends of the polepieces by passage of current of suitable strength and polarity through the coils. The coils were wound and interconnected so that current of one polarity would enhance the field strength at one end while diminishing the field strength at the other end. Current reversal has a reverse effect and moves the suspended mass in the opposite direction.

This design provided several advantages over the piezoelectric forcer system. The whole seismometer became more rugged by eliminating the somewhat fragile piezoelectric assembly. This improved its transportability significantly. Low voltages rather than high voltages (up to 100 volts) lessened insulation problems and simplified the electronics requirements. The substantial iron magnetic return paths outside of the coil assemblies in combination with the iron case of the instrument provided good shielding from external magnetic disturbances such as iron

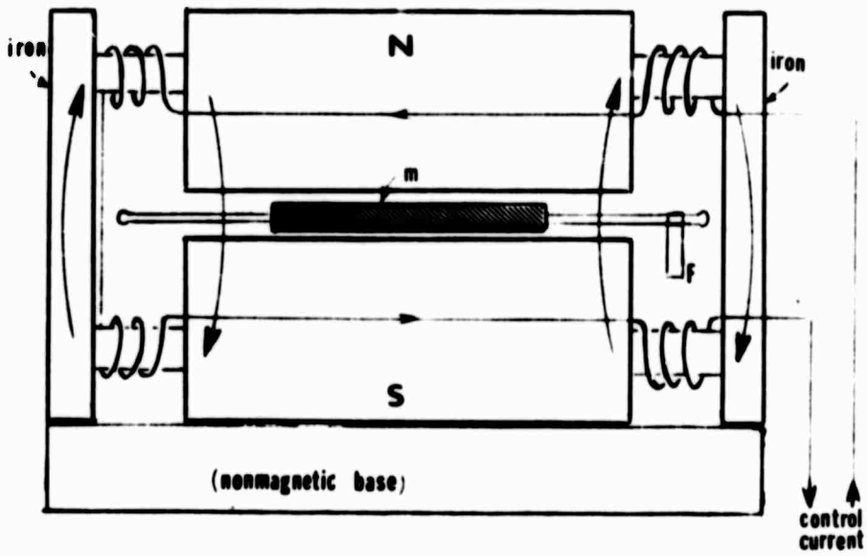

FIGURE 6 MAGNETIC FIELD FORCER FOR THE HORIZONTAL SEISMOMETER

borehole casings and stray fields. Simplifications in mechanical design lead to less expensive construction. The performance of the "magnetic" instrument was comparable to that of the "piezo-electric" instrument. The magnetically forced instrument was not thoroughly tested nor was the forcing coil structure optimized because of time limitations.

2. VERTICAL SEISMOMETERS

Theory of the vertical seismometer using magnetic field suspension was described in detail in the preceding annual report[6] and the present instrument designs were based on this theory. Figure 7 shows a schematic diagram including all essential parts of the seismometer. Photograph of the seismometer is shown in Figure 8. The seismic mass m, approximately 10 gms in weight, is an elongated cylindrical body, 0.187 in. in diameter, 8.50 in. long. In its middle it contains a short (0.15 in.) platinum-cobalt magnet which serves to levitate the seismic mass in neutral equilibrium. This is accomplished by a magnet assembly M generating a field of uniform gradient of a magnitude and direction such that the vertical force acting on the dipole N-S is exactly equal and opposite to its weight. The instability of the suspension is eliminated by providing frictionless guides at the ends of the seismic mass which take up any inverting torques arising from angular deviations of the suspended magnet from the vertical axis of symmetry of the magnet assembly M. The frictionless guides consist of two graphite rods g centered in the working gap of the quadrupole magnet assemblies Q_1, Q_2 by virtue of strong radial field gradient generated between the polepieces N-S. In this way the seismic mass assembly is restricted in its movement essentially in the axial direction and it can do so freely without making bodily contact with any part of the seismometer frame. The top of the seismic mass assembly carries a spherical lens which serves as a kinematic light switch between the lamp and the dual photocell in the electrooptical displacement sensor EO. Feedback control of the position of the seismic mass is effected by a pair of motor coils M_1, M_2 wound over the cylindrical permanent magnets in the magnet assembly M. The motor constant of these coils was, typically, 4000 dynes/ampere. Another pair of coils L_1, L_2 is used to provide for adjustment of the field gradient in the vicinity of the suspended dipole.

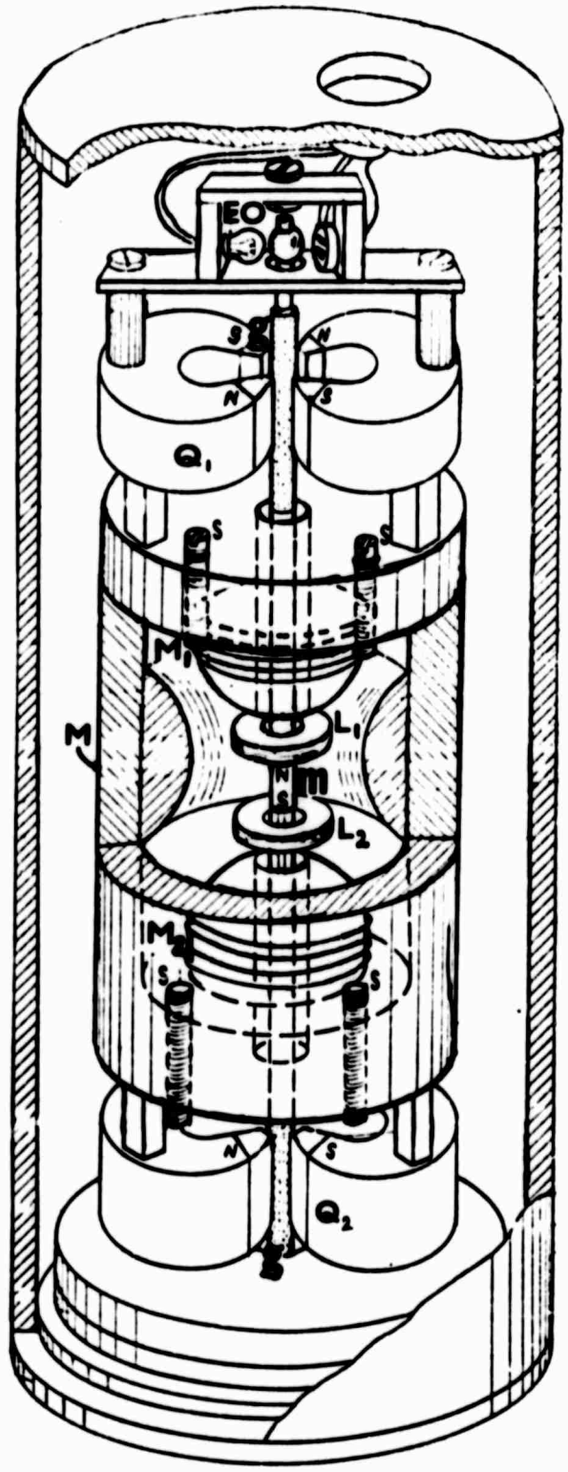

FIGURE 7 CUTAWAY VIEW OF THE VERTICAL SEISMOMETER
(Schematic)

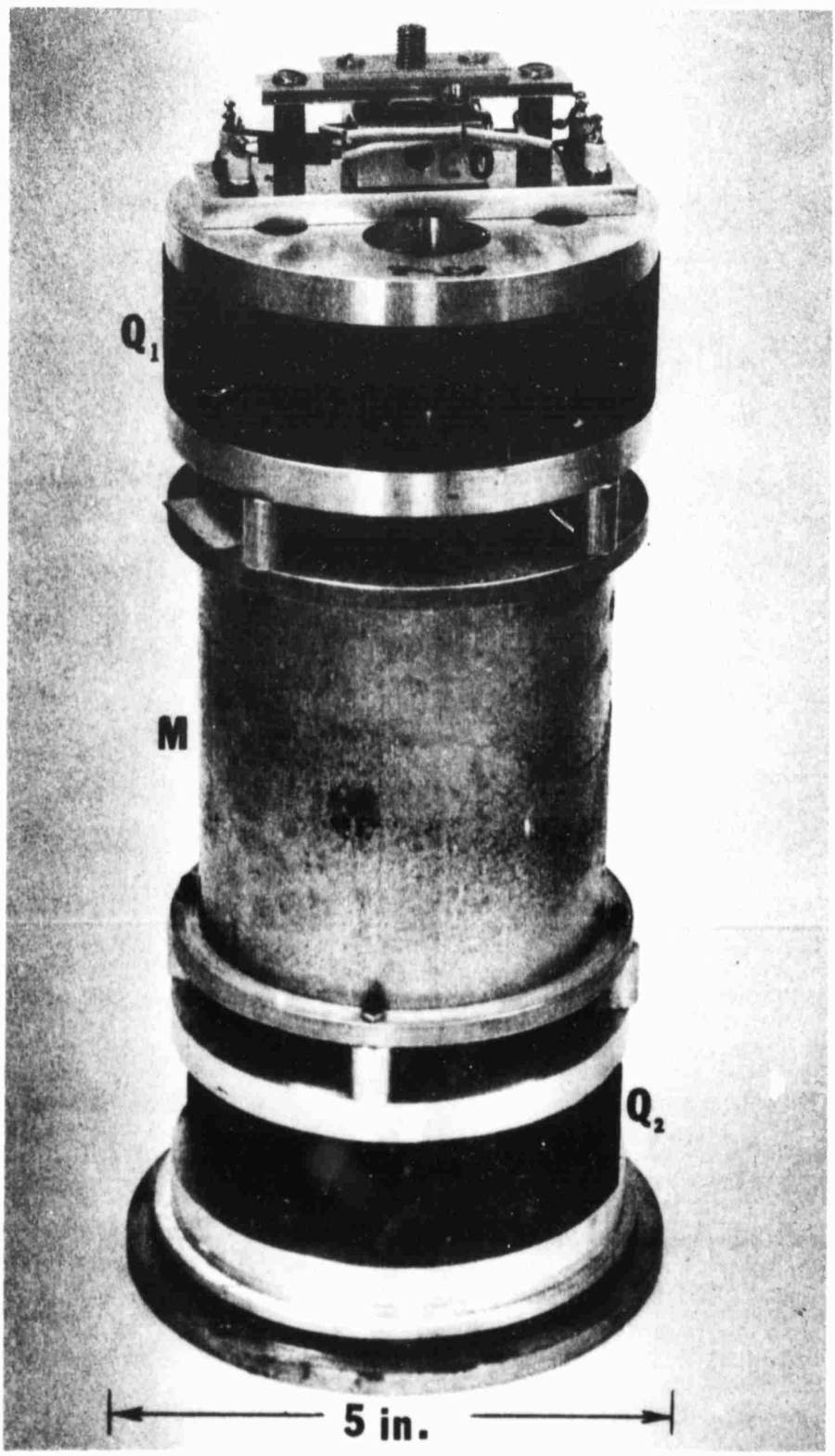

FIGURE 8 VIEW OF THE VERTICAL SEISMOMETER
(Photograph)

This adjustment is used to fix the natural period of the suspension. Rough adjustment of the overall field strength of the magnet assembly is made by means of flux shunt screws S.

In order to obtain the required long natural period ($T \geq 15$ sec.) of the magnetic suspension over the required range of displacements (approximately $\pm$ 1mm, depending on the optical sensor), the supporting field generated by the magnet assembly M must conform closely to the theoretical requirements derived in reference (6). For the axial field component H_z the requirement reduce to

$$H_z = H_o - \frac{W}{\mu} z + \frac{K}{\mu} z^2,$$

where $W = mg$ is the weight of the seismic mass, μ is the dipole moment of its magnet and K is the restoring force of the suspension ($K = 4\pi^2 m/T_o^2$). It has been also shown in reference (6) that the field satisfying this condition can be generated, in principle, by equipotential polepieces of the form of a hyperboloid of revolution with asymptotes defined by equation $z = \pm r/\sqrt{2}$.

In the actual construction of the magnet assembly the requirements of the theory can be satisfied only to a certain degree of perfection depending on the limitations of available space and properties of materials, such as finite permeability of iron etc. The restoring force $-\mu(\partial^2 H_z/\partial z^2)$ should be, according to the equation above, a linear function of z. In practice we found it to contain higher order terms, in particular quadratic, as can be seen from Figure 9. The quantity plotted is the measured residual F_z remaining after the first two terms of the force $\mu(\partial H_z/\partial z)$ have been cancelled out by adjusting the overall field gradient to a value necessary to levitate the seismic mass just above the center line of the magnet assembly ($z = 0$). With no current in the period adjustment coils L_1, L_2

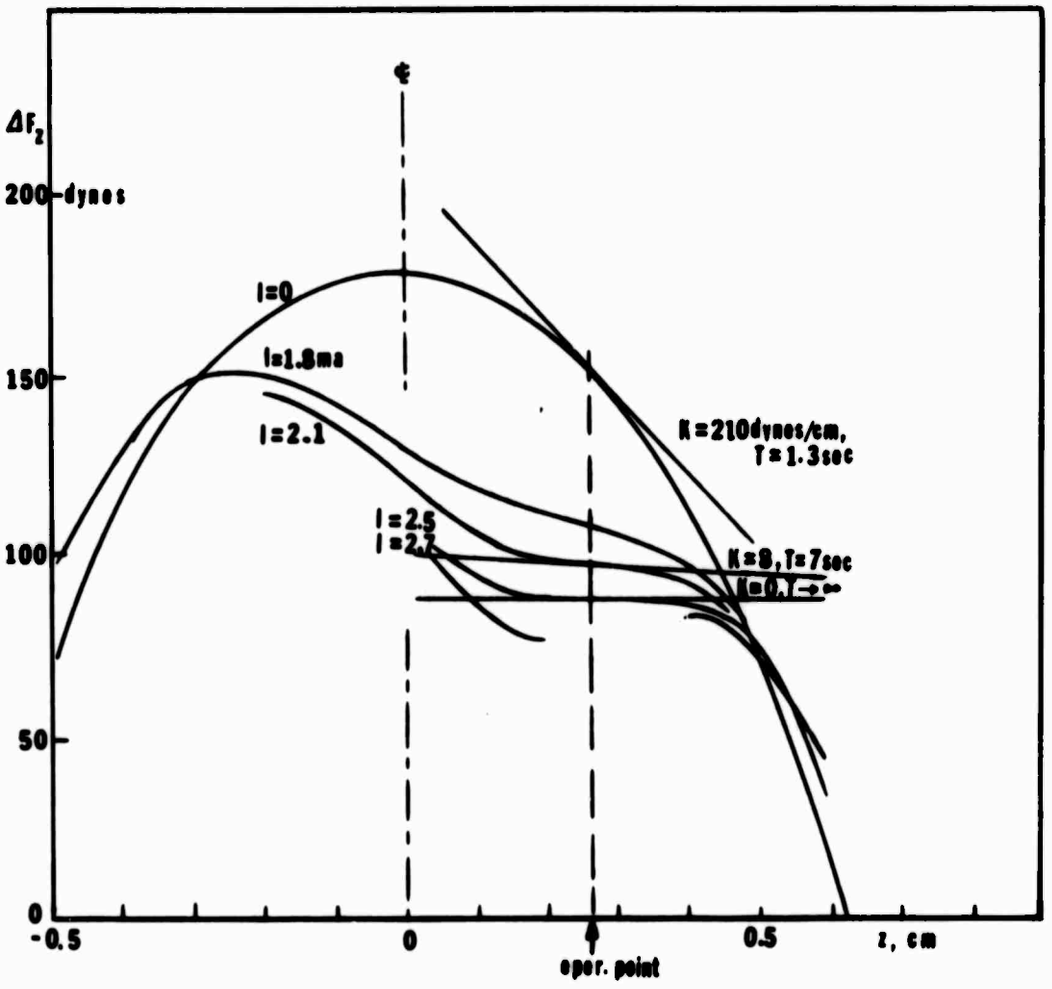

FIGURE 9 RESIDUAL OF THE MAGNETIC SUPPORTING FORCE IN THE VERTICAL SEISMOMETER AS A FUNCTION OF VERTICAL DISPLACEMENT

the force curve is approximately parabolic and the natural period of the suspension varies over a wide range depending on the location of the operating point above the center line. By applying suitable current to the L-coils the field in the vicinity of the suspended magnet is modified, resulting in residual force curves having a point of inflection as shown in Figure 9. Several curves are plotted for current values of 1.8, 1.9, 2.1, and 2.5 ma. At 2.5 ma the tangent is parallel to the z-axis and the period becomes infinite; beyond this value the period is imaginary and the suspension is bistable. In use the L-coil current is set and held at the selected value by a separate constant-current power supply.

Since the fields in the permanent magnet assembly M vary somewhat with temperature it is necessary to provide for appropriate adjustment of the gradient so as to hold the seismic mass at the operating point at all times. This is accomplished in the course of the overall feedback control as described below.

The circuit diagram of the vertical seismometer feedback circuit is shown in Figure 10. All amplifiers shown in the circuit are solid-state operational amplifiers. The feedback control is performed by amplifiers A_1 and A_2 in a circuit designed to have an overall transfer function of the form $K(s+a)/(s+b)$. Analysis of feedback with this transfer function indicated (6) that for adequate damping ($\delta \geq 0.7$) the gain must increase in a step of 1:16 for the bandwidth ratio a/b in order to allow for a possible 4:1 change of K with frequency. The gain and frequency of the gain step are adjustable over a range of approximately 1:20 and approximately 0.3 to 1.6 Hz, respectively, by the networks coupling amplifiers A_1 and A_2. The output current is fed back to the motor coil of the seismometer in a proper sense to drive it at all times to the null position defined by the optical displacement sensor. The voltage proportional to the

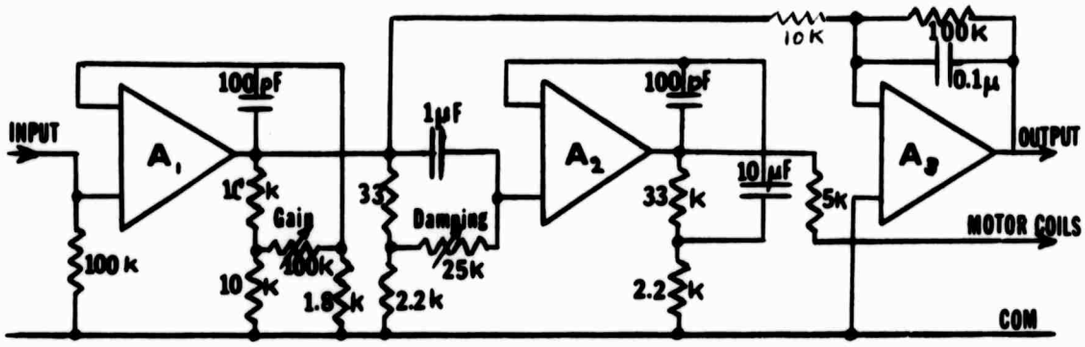

A_1: PP35C

A_2: PP25AU

A_3: PP85 AU (All Philbrick)

FIGURE 10 FEEDBACK CONTROL CIRCUIT OF THE VERTICAL SEISMOMETER

feedback current is amplified by A_3 which is provided with a small amount of low-pass filter characteristics (6db/octave above 1 Hz). The feedback loop includes an integration stage in the feedback loop of the amplifier A_2 which provides high gain at very low frequencies below the bass band of interest. This circuit adjusts the mean value of the feedback current to the motor coils to a d.c. value necessary to hold the seismic mass around its null position in spite of the drift in the magnetic suspension force caused by the effect of temperature, etc.

With the feedback loop closed the acceleration responsivity of the vertical seismometer is, typically, 10 volts per cm sec^{-2}.

3. FILTERS

Overall feedback in the seismometer results in a flat frequency response well beyond the natural resonant frequency of the mass-suspension system. Because the feedback element produces a force (rather than a displacement) the feedback seismometer delivers an output voltage proportional to acceleration. Filters are used in the output to produce a flat displacement response by virtue of a ω^{-2} response characteristics in pass band. Two-pole, controlled-source active RC filters[7] were used. The circuit, as shown in Figure 11, provides for passing the seismometer output through all three filter sections (displacement response) or only the last two sections (acceleration response).

The last section, A_3, is a 90-second corner frequency high pass filter used to limit the low frequency gain. This stage also provides a gain of ten. The middle section, A_2, is a twenty-second corner frequency low pass filter which limits the high frequency response of the output. An optional connection in this circuit provides an additional gain of ten. These last two sections used together provide a flat acceleration response from 90 to 20 seconds period.

The first stage is a unity gain low-pass filter with a forty-second corner frequency. The double integration of this two-pole filter converts the response for frequencies above forty seconds from proportional to acceleration to proportional to displacement. Thus, in the displacement position the response to displacement is flat from forty seconds to twenty seconds period. The asymptotic frequency response curve of the filter and the actually measured curve are shown in Figure 12.

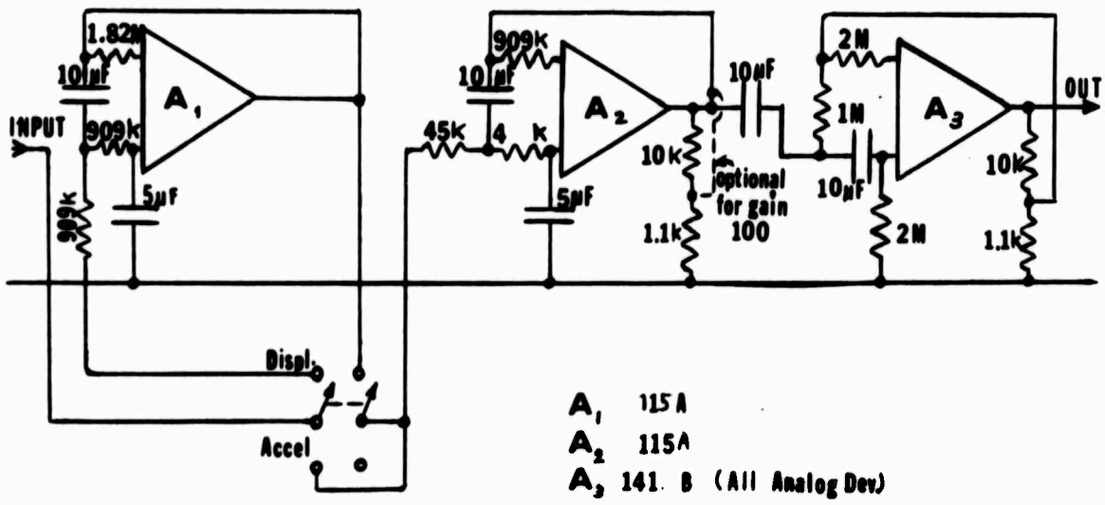

FIGURE 11 CIRCUIT DIAGRAM OF THE ACTIVE FILTER USED WITH THE FEEDBACK SEISMOMETERS

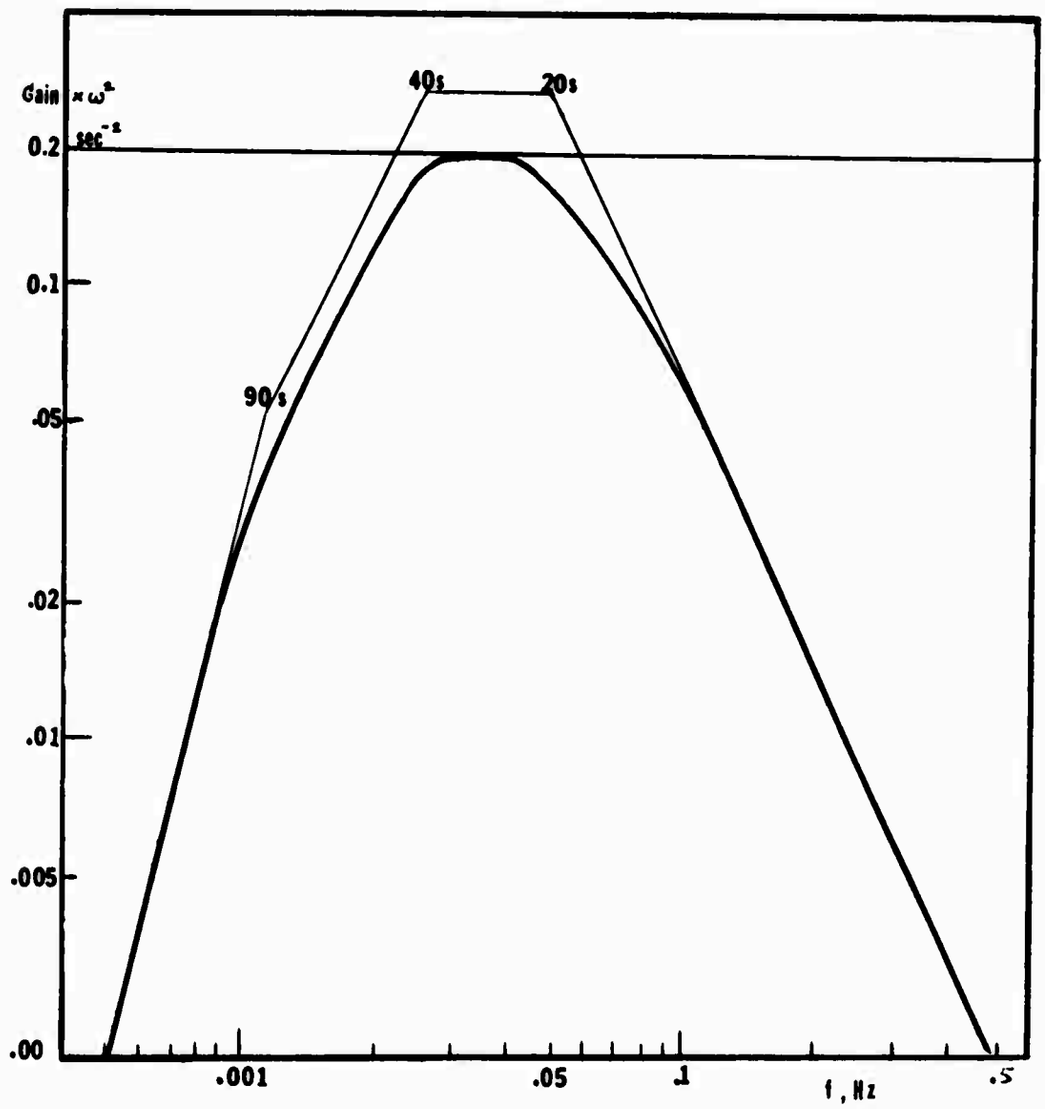

FIGURE 12 ASYMPTOTIC AND MEASURED FREQUENCY RESPONSE CURVES OF THE FILTER ACCORDING TO THE DIAGRAM OF FIGURE 11

The filters were identical for both horizontal and vertical seismometers. They were built in sets of three on a common panel with terminals for interconnection with the feedback control panels. Another panel contained a set of three variable gain (G = 1, 2, 5 and 10) amplifiers with flat frequency response. These were used for post-amplification when needed for the purpose of recording.

4. BOREHOLE PACKAGE

The seismometers were expected to be tested and used in boreholes of depth sufficient to minimize the deleterious effects of ground surface tilt "noise" and temperature fluctuations. While no theoretical background seems to exist for estimating the depth required to minimize the first-mentioned type of perturbations, the general practice is to use boreholes several hundred feet deep. The LASA LP seismometer holes drilled at the center of each seismometer cluster are 500 ft. deep (the SP seismometer holes are 200 ft. deep). At depths of this order thermal fluctuation, too, are greatly reduced. Calculation shows that in order to attenuate the daily temperature cycle to 5 percent of the surface value a steel-cased hole needs to be less than 10 feet deep; to accomplish the same attenuation for the yearly cycle, the necessary depth would be approximately 175 feet. Consequently, a borehole of this depth would provide nearly isothermal environment beneficial to the stable operation of seismometers.

No guidelines were given us as to the choice of the borehole diameter except the economic consideration. Depending on location, the cost of a finished, cased hole of 7 in. O.D. is approximately 15 to 20 dollars per foot and it increases more than proportionally with diameter. We chose the diameter of the borehole case header to be 6.00 inches O.D. so that it could fit a 6.50 inch I.D. casing typical of the central LP LASA boreholes. For the purpose of field tests we planned to drill a 75 foot deep borehole with steel casing of 6.50 I.D./7.00 O.D. on the grounds of the Harvard Observatory at Harvard, Massachusetts in cooperation with MIT's Department of Geology and Geophysics which operates a seismological station on the site. Unfortunately, because of redirection of test plans the hole was never drilled and the seismometers were tested in the Ogdensburg, New Jersey mine instead.

The overall view of the seismometer package is seen in Figure 13. The three seismometer units are joined together by turnbuckles and intermediate spacer rings permitting internal wiring to be brought up to the top header of the outer shell. The individual seismometer cases serve as pressure containers sealing off the instruments from any fluctuations of external pressure. The outer stainless steel shell serves principally as a watertight container protecting the interconnecting wiring and as a structural member mechanically connecting the three seismometers to the borehole by means of a hole lock. The whole package was to be lowered into and left resting at the bottom of a closed (cemented or welded) borehole casing. The hole lock would be sprung open upon release of tension on the stainless steel hoisting cable. Electrical cables would be left hanging slack in the borehole. The borehole was specified to be no more than 1.5° off the vertical and to be nominally dry.

Even if the borehole should fill with water the package and its O-ring seals were designed to maintain the seismographs dry against hydrostatic pressure of at least 50 psi (~100 feet depth). The inner steel cases, fabricated of tubing of 0.25 in. wall thickness, would actually sustain much greater external pressures. Elastic deformation of the cylindrical part of the seismometer case by external pressure is not prone to instabilities of the oil-can type which tend to plague conventional long-period seismometers installed in large pressure tanks. Actually, the only structural part of the case that would be critically affected by external pressure variations is the bottom plate which would deflect inwards and possibly tilt the seismometer mounted on it. However, for the dimensions of the base plate used in the present instrument (4.5 in. diameter, 0.5 in. thickness) such pressure deflections are extremely small (maximum deflection at center is approximately 4 microinches per psi). Moreover, the effect of the deflection is minimized by bolting the seismometer base to the case bottom plate symmetrically near its center where the slope is effectively zero.

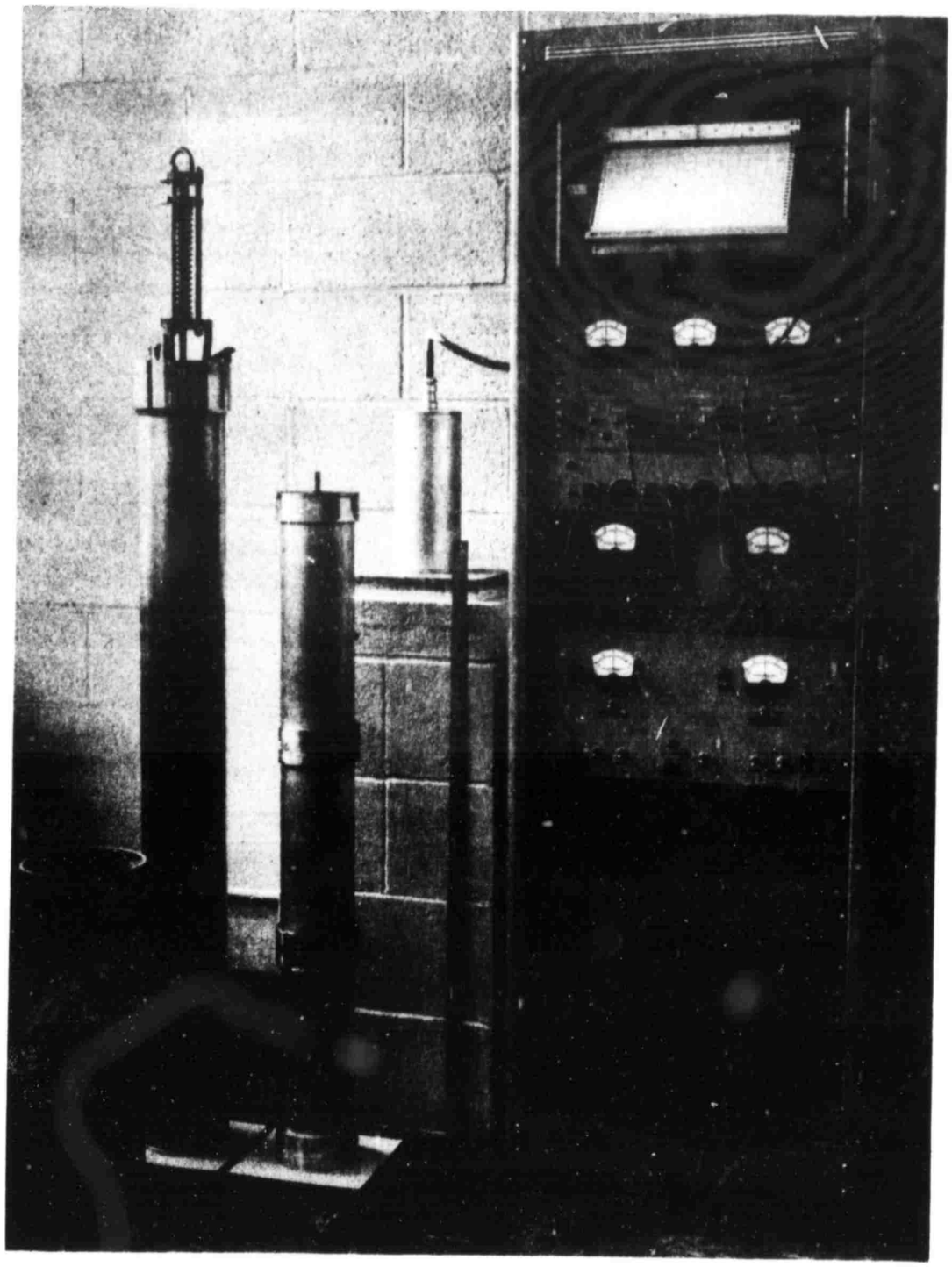

FIGURE 13 VIEW OF THE COMPLETE THREE-COMPONENT LONG-PERIOD SEISMOMETER WITH THE BOREHOLE PACKAGE. SECTION OF THE 6.5 IN. I.D. BOREHOLE CASING IS SHOWN ON THE LEFT. ONE OF THE HORIZONTAL SEISMOMETER UNITS IS ON THE LABORATORY PIER.

III. RESULTS OF TESTS

1. LABORATORY TESTS

a. Responsivity and Frequency Response

Responsivity and frequency response tests of seismometers complete with their servo control electronics were first made on laboratory piers. Because of the high ambient level of microseismic and cultural ground noise prevailing at the Cambridge, Massachusetts laboratory, tests had to be made at amplitudes large enough to make the effect of ground noise small compared with the test signal.

Ground noise was particularly troublesome with horizontal seismometers because of their high transducer responsivity. Most of their testing on the pier was performed on a long-base tilt platform by step-function input signals of the order of one-microradian (or one micro-g acceleration) in magnitude.

Vertical seismometers permitted testing by the more conventional methods (e.g., on a periodic lift table) because their sensitivity was considerably smaller than that of the horizontal seismometers. Their dc acceleration (gravity) response was determined by placing milligram weights on the top of seismic mass. Furthermore, because an additional motor coil was available in the vertical suspension system frequency response could be readily determined by injecting an electrical test signal of variable frequency in the motor coil. This was conveniently done by means of the Weston Servo Analyser (EMR Co. Mod. 1410); the same instrument was also used for determination of the frequency characteristics of filters such as shown in Figure 12 in the preceding section.

Typical characteristics of the horizontal and vertical seismometers established by these tests are summarized in Table I, below.

TABLE I

Horizontal Seismometers	
Period, free:	15 to 18 sec.
Period, with feedback:	2 sec. to inf.
Damping without feedback:	0.10 critical
Damping (feedback):	0.6 to 0.7 critical
Responsivity (with feedback):	2000 V sec^2/cm, (typ.)
Weight of inertial mass:	0.8 gm.
Vertical Seismometers	
Period, free:	10 to 12 sec.
Period, with feedback:	2 sec. to inf.
Damping without feedback:	0.08 critical
Damping (feedback):	0.6 to 0.7 critical
Responsivity (with feedback):	10 V sec^2/cm, (typ.)
Weight of inertial mass:	9 gms.

Responsivities of individual seismometers varied somewhat from the typical values given in Table I. They were determined for each instrument in the laboratory before the start of the field test program. Eleven weeks later, after the conclusion of field tests, the responsivities were rechecked in the laboratory and found to have remained within less than ± 5 percent of the original values.

The frequency response curves of the seismometers were quite uniform among the individual units. Typical frequency response curves of a vertical seismometer (VS-4) are shown in Figure 14 both for amplitude and phase. These curves were determined by the servo analyzer method mentioned above and they apply to the seismometer alone, without filter.

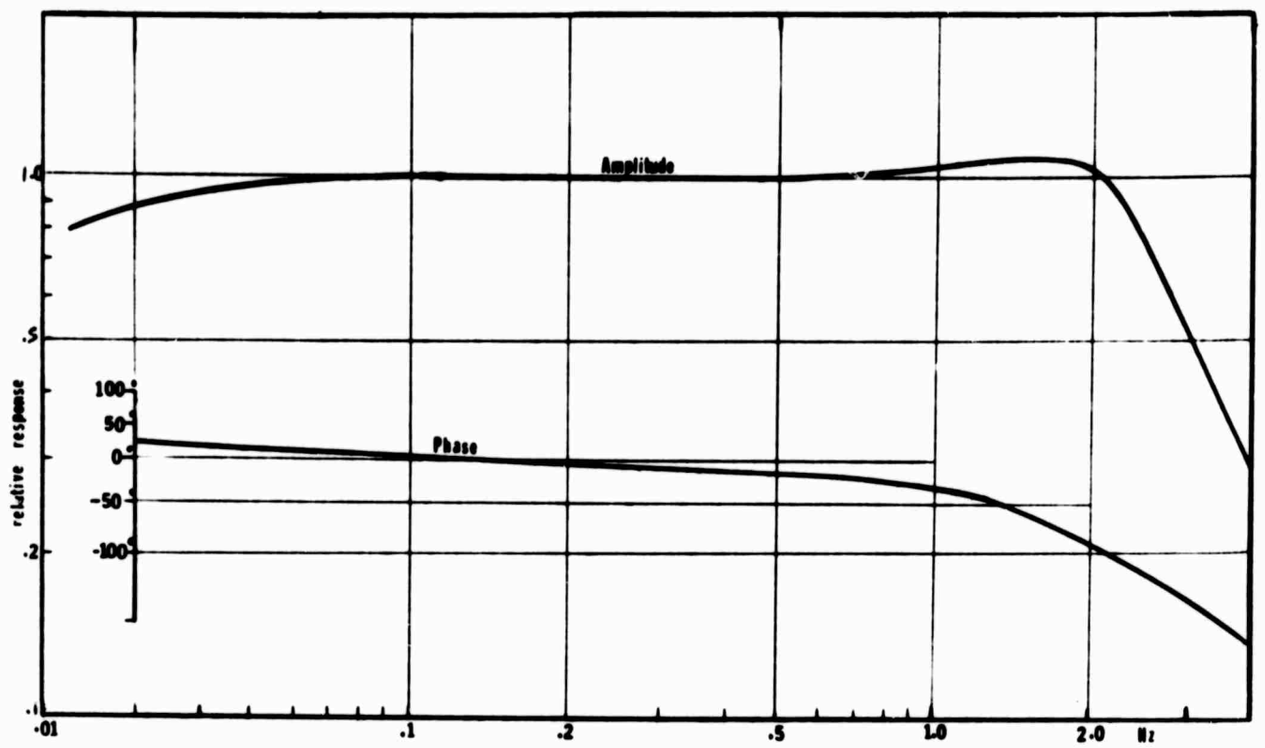

FIGURE 14 FREQUENCY RESPONSE CURVE OF THE VERTICAL FEEDBACK SEISMOMETER (WITHOUT FILTER) MEASURED WITH A TEST CURRENT OF CONSTANT AMPLITUDE AND VARIABLE FREQUENCY INJECTED INTO THE MOTOR COIL

Frequency response of the same seismometer determined by the mechanical periodic lift table of constant amplitude (17 microns peak to peak) is shown in Figure 15. In this test the seismometer was used with the flat displacement response filter (Section II-3) since with the periodic lift table the displacement rather than acceleration is kept constant. The filter with gain proportional to ω^{-2} modifies the output of the seismometer to a voltage directly proportional to displacement. Since the mid-band gain of the filter was 0.2 the displacement responsivity of the seismometer was 2V/cm. The experimental points are plotted over the asymptotic response curve of the filter (compare with Figure 12). The large scatter of the experimental points is caused mainly by the imperfections of the mechanical drive of the lift table; nevertheless, the conformance of the experimental points with the design curve appears to be within the limits of experimental error.

b. Cross Coupling

The cross input responsivity of the seismometers was determined by testing the vertical instruments on the horizontal translation table and vice versa. Results of these tests were only of a qualitative value since the mechanically operated tables generated rather large cross signals of uncertain magnitude. We could only estimate that the responsivity of vertical seismometers to horizontal displacements was at most about 5 percent of that along vertical axis. This maximum was obtained when the horizontal movement was in the direction normal to the optical axis of the electrooptical displacement sensor; when the movement was along the direction of the optical axis the cross responsivity was effectively zero. Similar tests attempted with horizontal seismometers were far less conclusive because the mechanical lift tables produced excessive spurious tilts.

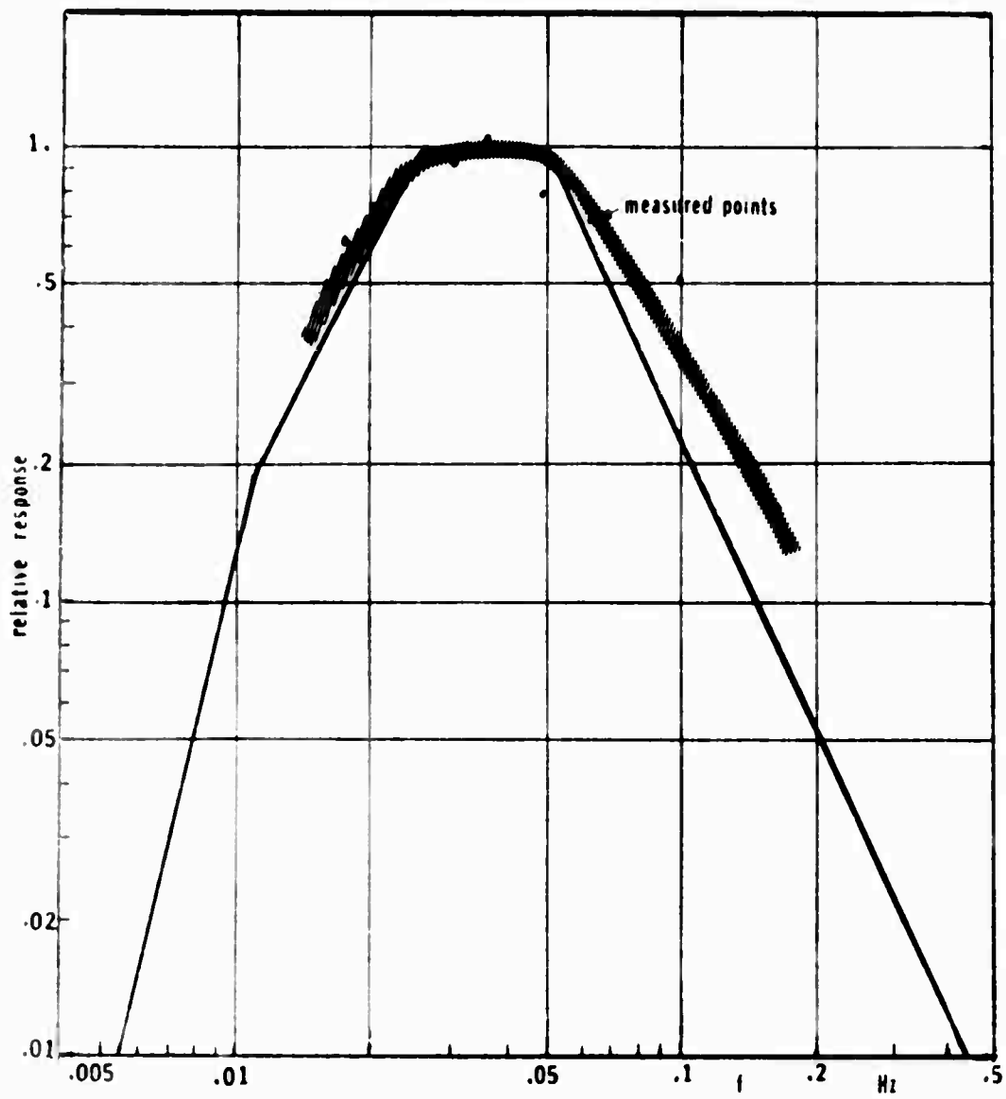

FIGURE 15 FREQUENCY RESPONSE CURVE OF THE VERTICAL FEEDBACK SEISMOMETER (WITH FILTER) MEASURED ON A VERTICAL LIFT TABLE AT CONSTANT DISPLACEMENT

c. External Magnetic Fields

Because of the nature of the magnetic suspension used in the seismometers there was a legitimate concern about the effect of external magnetic fields on the instruments. Moderate magnetic fields (of the order of a few gauss) have no measurable effect on the responsivity and frequency response of the seismometers, but they can produce spurious signals. In case of the vertical seismometer any external field producing a gradient in the vicinity of the suspended dipole generates a force acting on the seismic mass and thus a spurious signal. This first-order effect can be only reduced by shielding. Shielding was provided in the present instruments by the pressure container made of magnetically soft steel. With wall-thickness-to-radius ratio equal 0.11 and relative permeability $\mu \geq 1500$, the calculated attenuation ratio of the external field by the container was approximately 100.

In normal use the seismometers would not be expected to see external field greater than approximately one gauss (earth's field). Such a field, if constant, would be of little consequence; only if it varied on a time scale comparable with that of the seismic signals it would constitute interference. By actual tests in the laboratory with a recording magnetometer placed near the vertical seismometer we found that interference by variable external fields became comparable to the seismic signals (ground noise) when the external field amplitude exceeded approximately one milligauss or 100γ. Earth's field fluctuations only rarely exceed 50γ peak-to-peak and their period is typically hours rather than minutes; hence, their effect should be negligible.

Similar observations apply to the horizontal seismometers. Here, however, because of the smallness of the diamagnetic magnetization in the suspended mass external magnetic field exerts a force at least five orders of magnitude smaller than in the

vertical seismometer. In this case the perturbing force arises from the change of the overall strength of the suspension field and only when the diamagnetic seismic mass is suspended asymmetrically from the transverse mid-plane of the polepiece structure. Asymmetry may be caused e.g., by a departure of the optical read-out block from the proper position. By micrometric positioning of the optical block with respect to the polepiece structure the effect of the external field can be minimized and essentially eliminated. This was discovered only after the completion of the seismometer development and construction. Consequently, horizontal seismometers as tested, were found to be affected by external magnetic fields to approximately the same degree as the vertical seismometers.

d. Effect of Temperature

Temperature variations tend to shift the central position of the seismic mass both in the vertical and horizontal seismometers. In the vertical seismometer the feedback control counteracts the effect of temperature as long as the integrating amplifier A_2 (Figure 10) can deliver a control current of a mean value sufficient to hold up the suspended dipole at the operating level. This is possible over a range of approximately 5°C by a variation of the control current of typically 1 ma per °C. If larger temperature departure from the initial value is encountered it can be corrected by adjustment of one of the flux shunt screws S shown in Figure 7.

In the horizontal seismometers the mean position of the seismic mass can be held by feedback control only over a rather small temperature interval because of the limited range of the piezoelectric tilters. This range was found to be of the order approximately 1°C. When a larger temperature change occurs the seismic mass may escape the control and repose against one of the end stops. In this case the automatic leveling circuit (as shown in Figure 5) actuates the motor-driven jack screw which restores the seismic mass to its initial position.

2. SEISMIC TESTS

Seismic field tests were performed during the period from February 5 to March 24, 1969 in cooperation with Lamont-Doherty Geological Observatory at the Observatory's sites in Sterling Forest, New York and Ogdensburg, New Jersey. The tests were planned to serve the following purposes:

To determine the performance limits of the seismometers at a site of ground noise level substantially lower than at our laboratories.

To obtain data that would permit separation of the observed noise in the internal (instrumental) and external (microseismic) components by inter-comparison of individual seismometers.

To compare the detection capability for small teleseismic events of the ADL Seismometer System with that of the Lamont High-Gain, Wide-Band Long-Period System[3] and the Lamont OBS System[8]; and,

To demonstrate the capability of the ADL system to operate under field conditions (deep mine).

a. Description of Systems, Sites and Installation

The ADL equipment under test consisted of two complete three-axis seismometer systems, feedback control electronics, filters, amplifiers and recorders (4-channel chart recorder and 16-channel digital tape recorder). The system was described in the preceding sections and its transducers characterized in Table I. The block diagram of the complete ADL system is shown in Figure 16. The seismometers in the vault were connected by 50 ft. long cables to a rack containing all feedback control

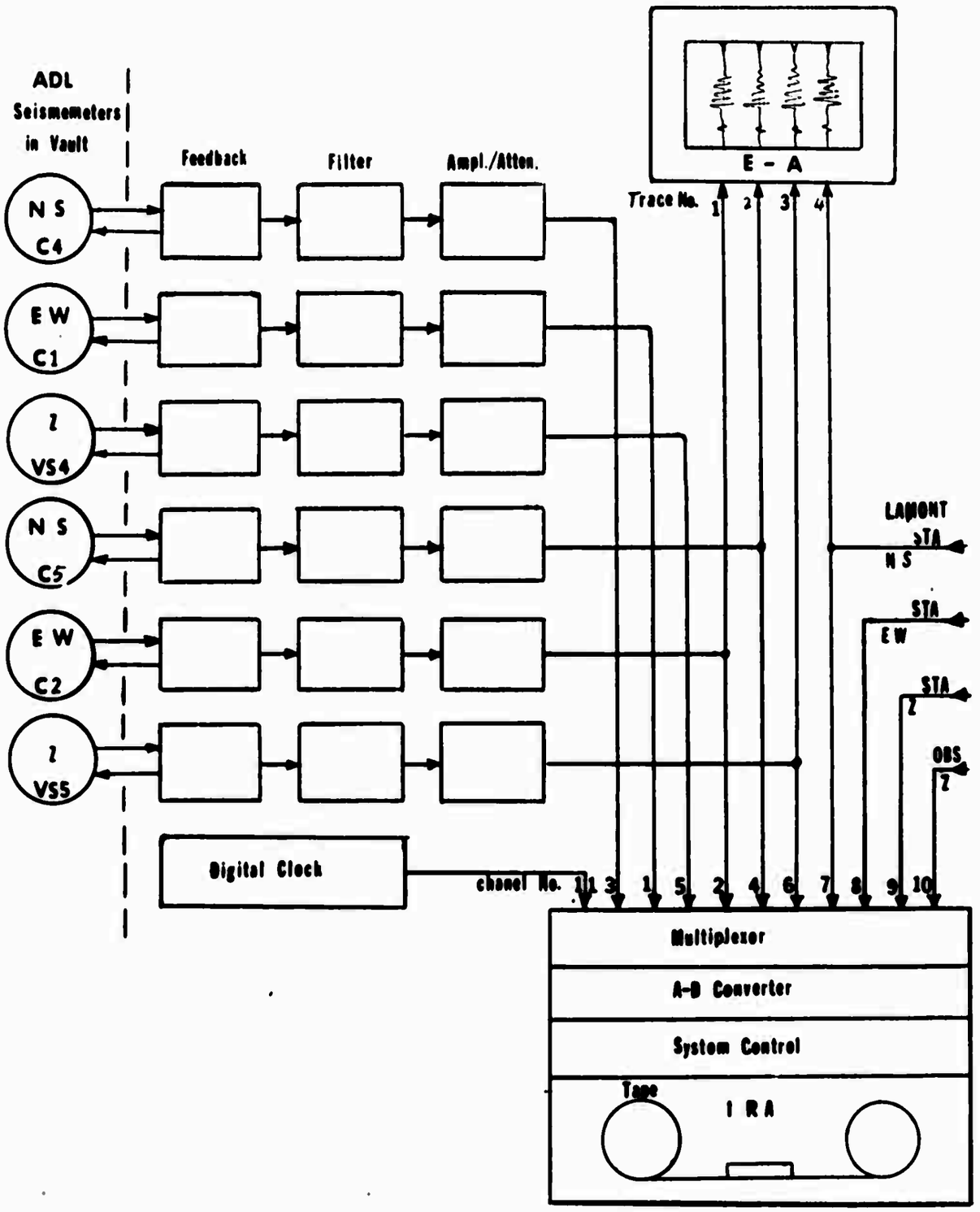

FIGURE 16 BLOCK DIAGRAM OF THE COMPLETE ADL SYSTEM USED FOR SIMULTANEOUS TESTING OF SIX ADL SEISMOMETERS AND RECORDING OF FOUR ADDITIONAL OUTPUTS OF THE LAMONT SYSTEMS

electronics, filters, amplifiers and the Esterline-Angus chart recorder. Numbers C4, VS4, etc., shown in Figure 16 refer to the designations of the individual ADL seismometers.

The Lamont Observatory's High-Gain, Wide-Band Long-Period System[3] (henceforth called STA) comprised one vertical seismometer, Geotech Model S-11 and two horizontal seismometers, Geotech Model S-12, with 100 sec. galvanometers, phototube amplifiers and filters. The principal characteristics of both vertical and horizontal seismometers were as follows:

Natural Period:	30 sec. (typ.)
Damping:	electromagnetic, critical
Sensitivity (Catalog value):	11.7 V/m at 15 sec.
Weight of inertial mass:	10 kgms.
Motion transducer:	electromagnetic (velocity)

The Lamont Observatory's Long-Period Feedback System[8] (henceforth called OBS) consisted of a unit containing three orthogonal seismometers, the feedback control electronics, filters and amplifiers. The principal characteristics of the system were as follows:

Natural period:	15 sec.
Sensitivity:	250 V/micron (Max.)
Weight of inertial mass:	1.5 kgm

(only z-component signal was available during tests.)

The frequency response curves of the three complete systems are compared in Figure 17. Both of the Lamont Systems have a steeper cutoff at the short period side than the ADL system. Moreover, the Lamont STA system was provided with a -40 db notch filter for suppression of the 6-sec period microseisms. Some of the data recorded by the ADL system were subsequently high-pass filtered by a computational algorithm; this is indicated in the frequency response curve by the dashed line.

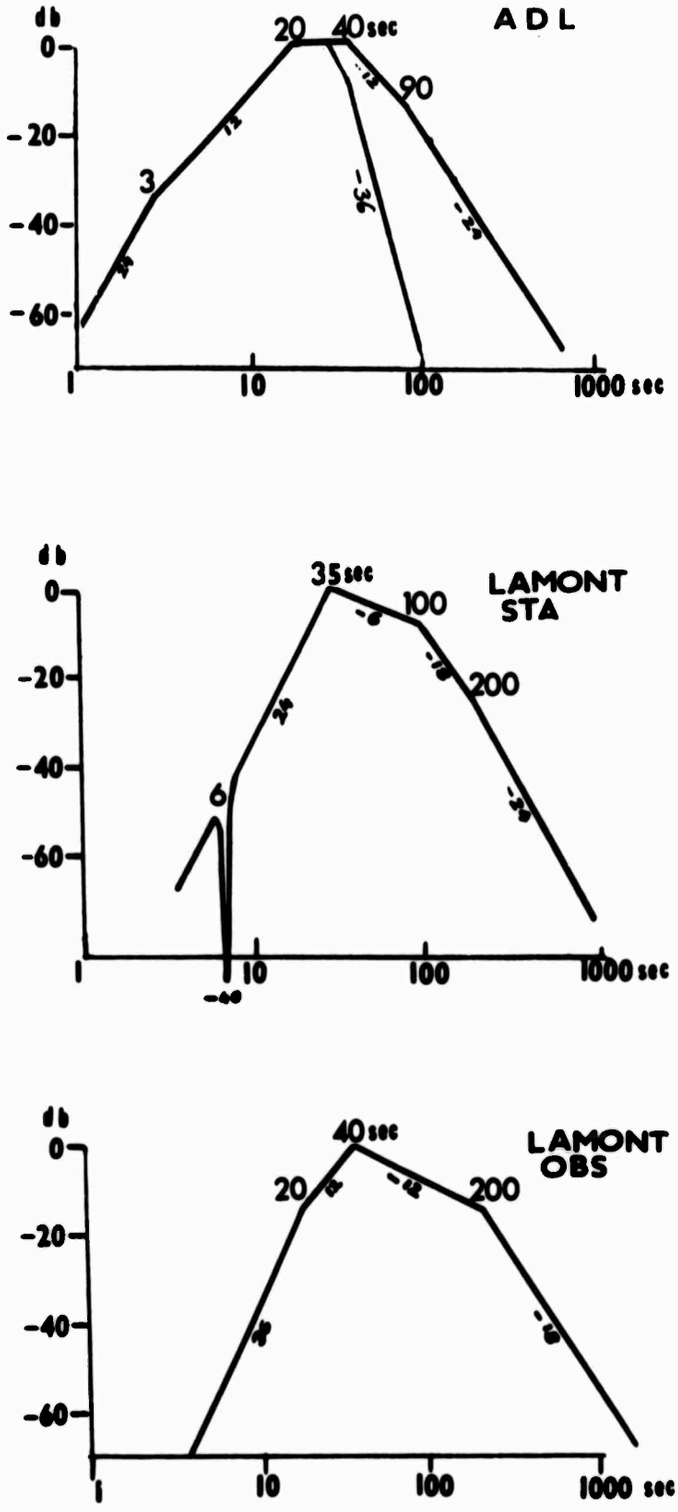

FIGURE 17 ASYMPTOTIC FREQUENCY RESPONSE CURVES OF THE THREE SEISMOMETER SYSTEMS UNDER COMPARATIVE TESTS AT THE OGDENSBURG SITE

Data from all ADL and Lamont seismometers (10 channels and GMT time from a digital, crystal-controlled clock) were recorded by a digital tape recorder (IRA Model 710) at sampling rates from 3 to 30 per second. This permitted continuous recording (on 1200 ft. tape reels) over time intervals from 2 days to three weeks depending on sampling rate.

The Lamont Advanced Long-Period System (STA) was found to have performance (in terms of sensitivity and signal-to-noise ratio) superior to both the ADL and the OBS systems. It is to be noted, however, that this was a station type instrument requiring elaborate installation in air-tight tanks in a vault cut in solid rock underground. The ADL system was developed specifically as a compact instrument designed for convenient installation in boreholes. This is best appreciated by comparing the size of the two instruments as shown in Figure 18. The Lamont OBS system is intermediate in size between the two extremes.

During the tests performed at Sterling Forest from 5 to 17 February 1969 it became apparent that the shallow surface vault in which the seismometers were installed suffered from excessive ground motions. The horizontal long-period seismographs of the Lamont System installed in the same vault were actually inoperative for this reason; only the vertical seismometer output was available for comparison. Because of the extremely high level of microseisms occasioned by stormy weather the tests were inconclusive and will not be reported here. Meanwhile, permission was granted by the New Jersey Zinc Company for ADL to use the Lamont facility and the equipment was moved to Ogdensburg, New Jersey of 17 February 1969.

The underground seismological station of the Lamont-Doherty Geological Observatory is located in Ogdensburg, New Jersey, (41°05'N, 74°35'W) at the 1850 foot level of an inactive

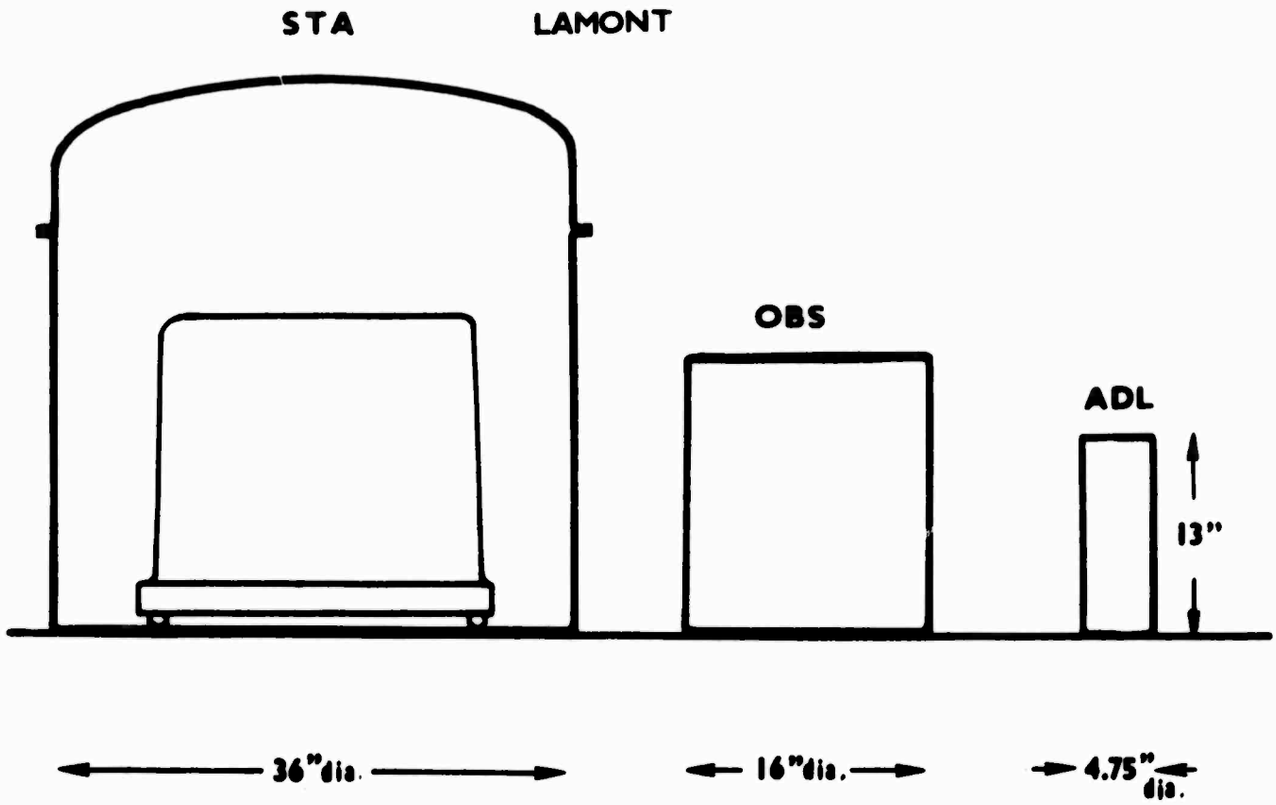

FIGURE 18 COMPARISON OF PHYSICAL SIZE OF THE THREE LONG-PERIOD SEISMOMETERS

tunnel of the New Jersey Zinc Company's mine. The space made available to us was in a fore-vault in front of the vault containing Lamont's STA system; Lamont's OBS seismometer was located in the same fore-vault as the ADL system. Instruments were placed directly on the rock base in a large niche in the side of the wall (Figures 19 and 20). The electronic equipment and the recorders were set up in a room separated from the fore-vault by double air-lock doors. The site proved to be highly satisfactory and we operated the system there until 25 March 1969.

For transportation of the system to the test sites the seismometers were crated in wooden boxes with their seismic masses clamped (vertical instruments) or temporarily removed (horizontal instruments). All equipment was moved by truck without any special precautions. Total mileage over which the ADL system was transported without harm was 520 miles. All equipment functioned properly upon installation at both sites. The environmental conditions at the Ogdensburg site were particularly severe because of the combination of freezing temperatures at the surface and extremely high humidity underground. As a consequence, all electronic equipment became saturated with condensed water. The seismometers, contained in their watertight steel casings were not affected by this and operated normally after equilibrating with surroundings. Likewise, all electronics, cables and recorders functioned normally after they had been allowed to dry overnight. Equipment was re-checked again after return to the laboratory in Cambridge and found to operate normally. Calibration of the vertical and horizontal seismometers was found to be within a few percent of the original values.

b. Results of Tests

During the tests the ADL system was operated for a total of 38 days (over 900 hours) continually, with a single

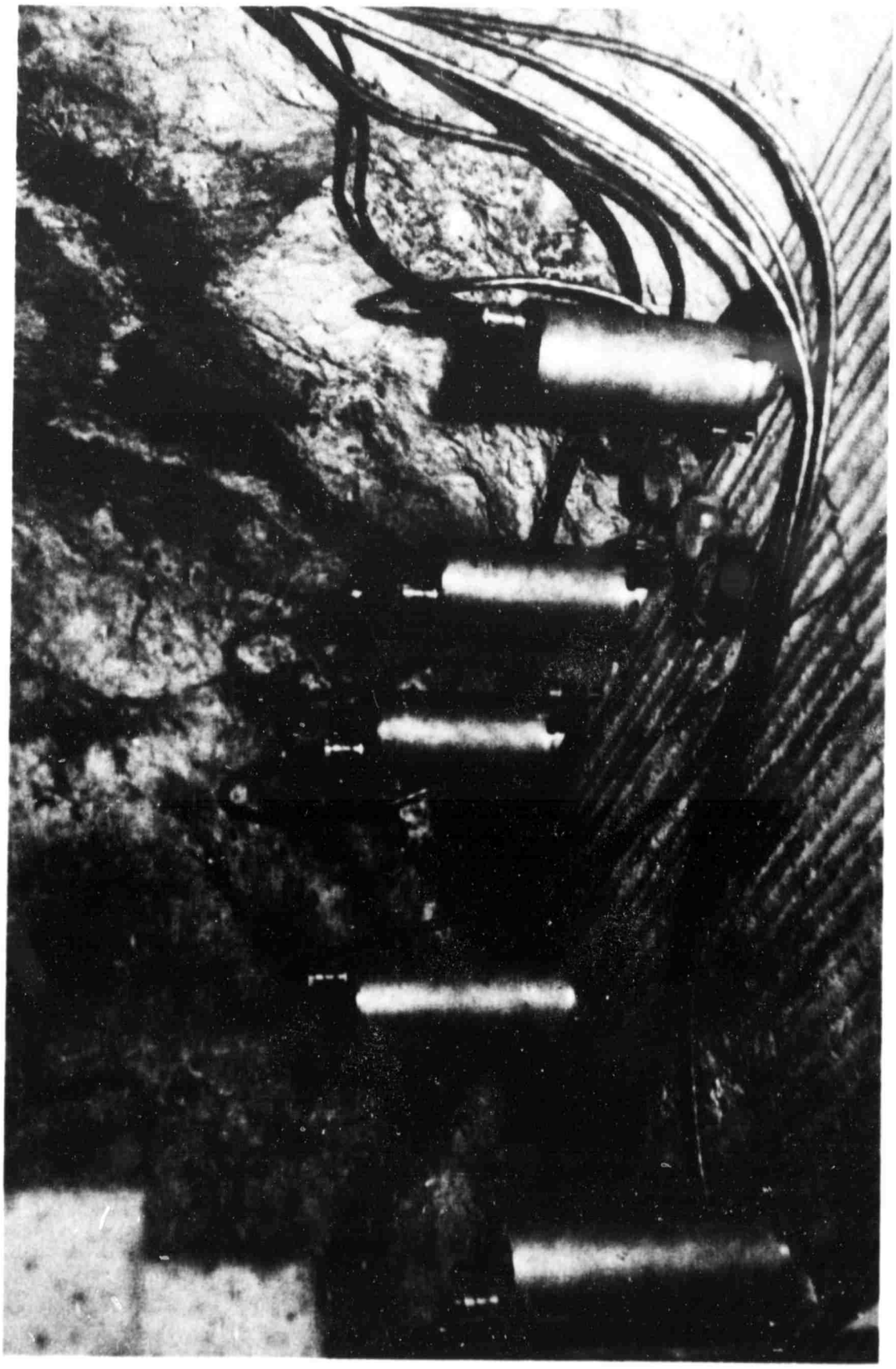

FIGURE 19 ADL SEISMOMETERS IN THE FOREVAULT AT THE OGDENSBURG, NEW JERSEY TEST SITE

FIGURE 20 ADL SYSTEM'S ELECTRONIC CONTROLS (LEFT) AND THE DIGITAL TAPE RECORDER (RIGHT BOTTOM) IN THE MINE

interruption at the time when it was being moved from Sterling Forest, New York to Ogdensburg, New Jersey. The seismometers, the electronics and the recorders functioned without failure during the entire test period, as well as after it was returned to Cambridge. Much of the time the system operated unattended. Occasionally, the operating voltages and currents were checked and at such occasions the horizontal leveling of the seismographs was adjusted. Even though the instruments were provided with self-leveling circuits one of the horizontal instruments failed to relevel itself on one occasion and remained inoperative for some time. The vertical seismometers stayed within their operating range during the entire test period. The temperature in the vault was found to remain constant within a few tenths of a degree around 18°C.

During the last week of tests tape records were changed daily through the kind cooperation of Lamont personnel. This was done in order to operate the tape recorder at the maximum available sampling rate (30 per sec.) so as to obtain data for subsequent processing (plotting, computation of means, cross-correlations and digital filtering).

During the tests at Ogdensburg approximately 100 seismic events of various magnitudes were noted on the monitor chart recordings. A number of these were subsequently identified from the P.D.E. cards published by Coast and Geodetic Survey or from the LASA Seismological Bulletin.

Selected recordings presented in the following were plotted from the digital tape record in a format permitting visual comparison between the ADL and Lamont systems. Most of the plots are in terms of ground displacement (in microns). For the ADL system the displacement scale is based on actual calibration of each individual seismometer. For the Lamont

system, the original scale was in volts, as at the time of writing calibration data were not available. We converted it to microns by comparison with the ADL system at 30 sec. period.

No effort was made to present the data on a high resolution time scale or at large displacement mganifications since this would permit to show only a very small segment of data at a time. However, the plotting program allows plotting of data from the magnetic tapes at any desired magnification or time scale. From the numerous records we present only a few typical examples which are discussed in the following.

Figure 21 is a reproduction of a computer plot from the digital recording of a teleseismic event originating at a distance $\Delta = 140°$ (Taninbar Island Region, 6.2°S, 131.0°E) at 00:08:46 GMT on 24 February 1969. CGS magnitude reported in the PDE cards was m_b=5.9. The two traces shown in the figure are placed side by side to permit comparison between one of the ADL seismometers and the Lamont STA seismometer; both were horizontal, East-West direction. The agreement appears satisfactory considering the larger background instrument noise in the ADL seismometer. Phases indicated in all figures were identified by means of standard travel time diagrams. No claim is made as to their absolute accuracy.

Recording of another teleseismic event is shown in Figure 22. This event occurred in the Fiji Islands Region (15.5°S, 176.1°W) at 05:43:57.5 GMT on 22 March 1969, the distance was $\Delta \approx 108°$, CGS magnitude reported in PDE cards was m_b=5.4. Comparison between the ADL and STA traces indicates a good agreement in all recorded phases; note the discrimination between L and R phases based on a high degree of transverse polarization of the Love waves in horizontal plane.

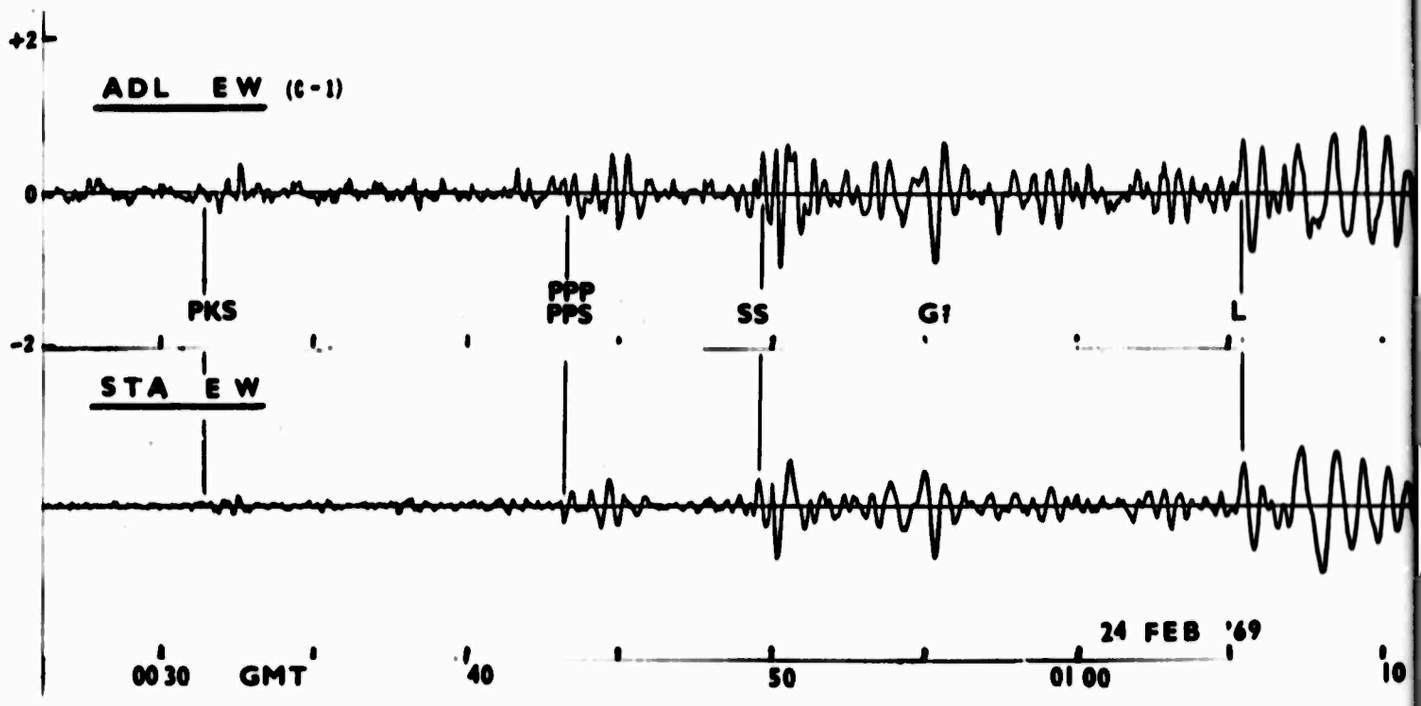

FIGURE 21 SAMPLE OF COMPUTER PLOTS OF
(m_b = 5.9; Δ = 140°; TANINBAR ISL
ORIGIN TIME 00:08:47, 23 FEBRUA
THE ADL AND LAMONT SYSTEMS

A1

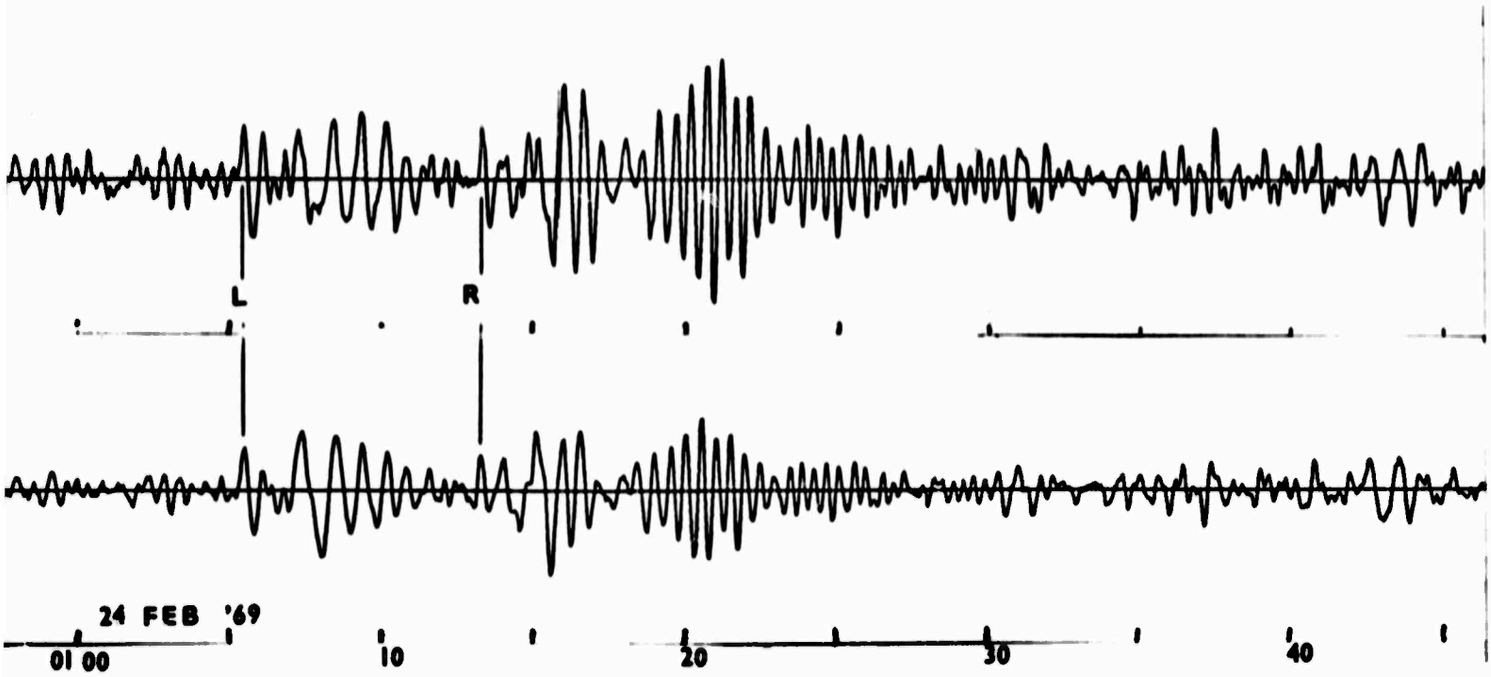

MPLE OF COMPUTER PLOTS OF A TELESEISMIC EVENT
, = 5.9; Δ = 140°; TANINBAR ISLAND, 6.2°S, 131.0°E;
IGIN TIME 00:08:47, 23 FEBRUARY 1969) RECORDED WITH
E ADL AND LAMONT SYSTEMS

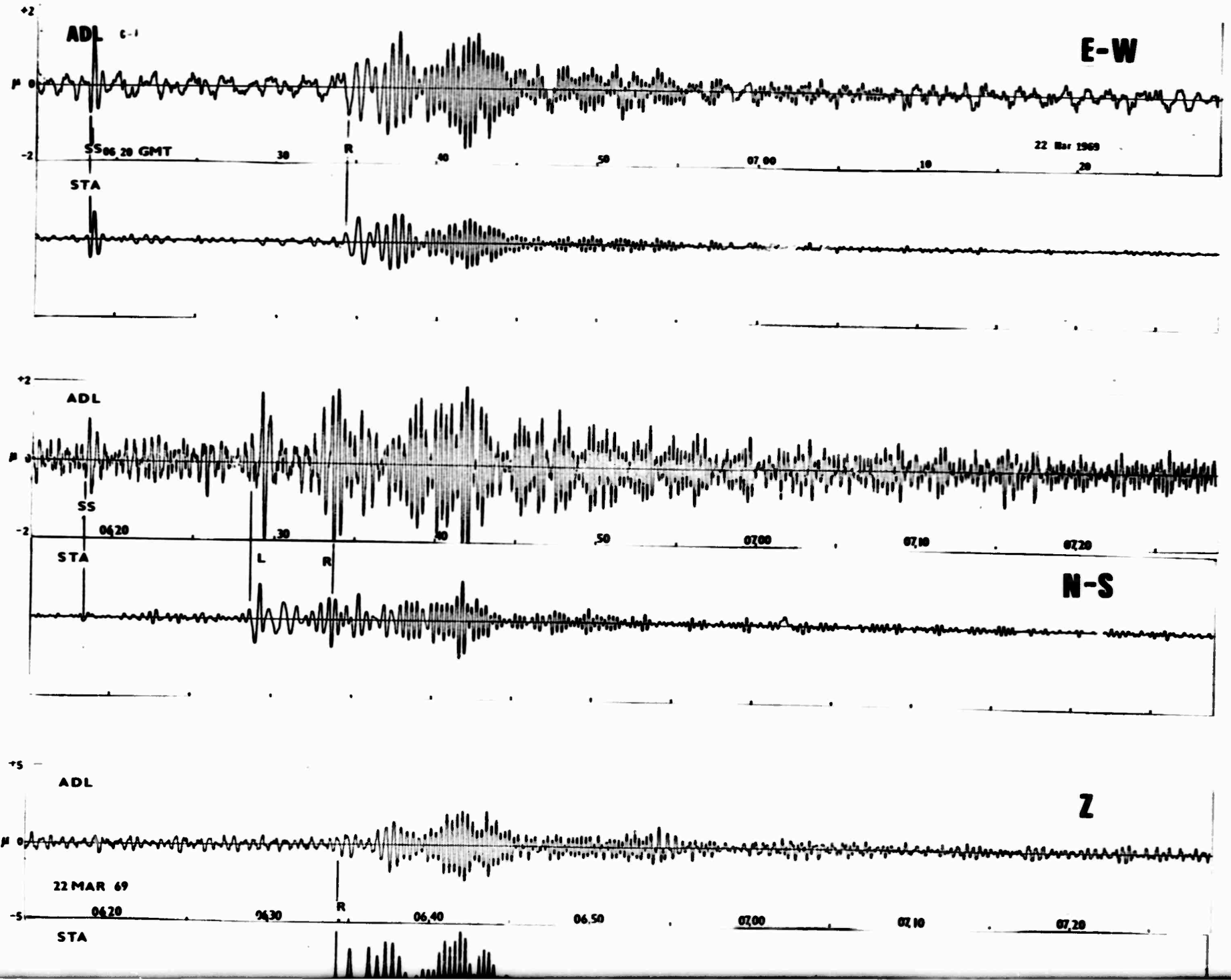
ADL
E-W
SS 06,20 GMT
30
R
40
50
07,00
10
20
22 Mar 1969
STA
ADL
SS
06,20
30
40
50
07,00
07,10
07,20
STA
L
R
N-S
ADL
Z
22 MAR 69
06,20
06,30
R
06,40
06,50
07,00
07,10
07,20
STA

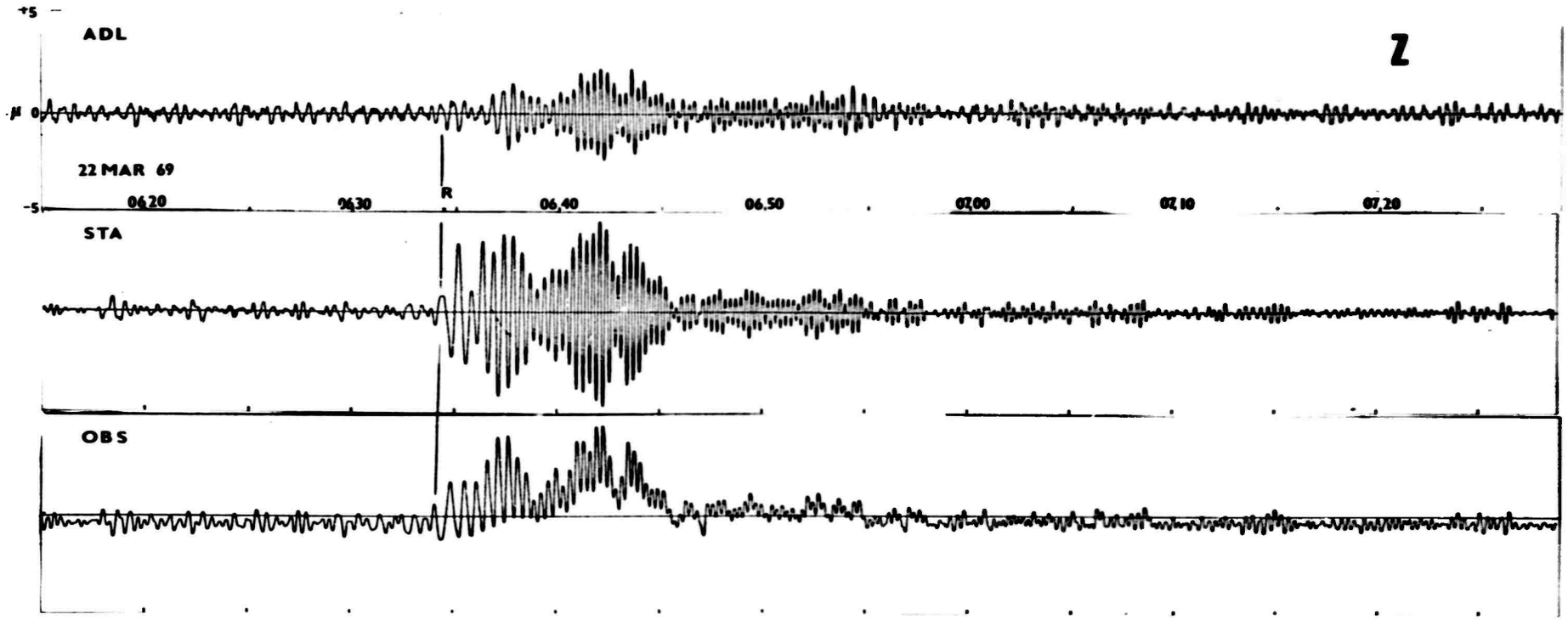

FIGURE 22 SAMPLE OF COMPUTER PLOTS OF A TELESEISMIC EVENT (m_b = 5.4; Δ = 108°; FIJI ISLANDS REGION, 15.5°S, 176.1°W; ORIGIN TIME 05:43:58, 22 MARCH 1969) RECORDED WITH THE ADL AND LAMONT SYSTEMS. THE N-S AND Z PLOTS OF THE ADL RECORDS HAVE BEEN DIGITALLY FILTERED. NOTE THE SEPARATION OF THE R AND L PHASES BY THEIR POLARIZATION.

In comparison with the Lamont STA seismometers ADL instruments appear to be considerably more noisy. As the E-W trace in Figure 22 indicates the dominant frequency of the ADL System noise appears to be between 0.01 and 0.02 Hz (50 to 100 sec. period). Consequently, it should be possible to reduce its magnitude by high-pass filtering without affecting the seismic signals in the 0.025 to 0.04 Hz domain. The N-S and Z outputs of the ADL system reproduced in Figure 22 were actually filtered in this way (the E-W record was not filtered). The digital filter had a high-pass response equivalent to a four-pole Butterworth filter with cutoff frequency f_c = 0.03 Hz and 24db/octave slope on the low-frequency side of the response curve.

The filter algorithm permitted the variation of the cutoff frequency without changing the slope. The effect of varying f_c on the appearance of a seismic record is illustrated in Figure 23. The event is the same as in Figure 22 and the top trace is unfiltered. The following two traces were high-pass filtered with f_c = 0.05 and 0.03 Hz. At f_c = 0.05 Hz the record of all long-period phases is acceptable, but at f_c = 0.03 Hz the long-period S and L phases are severely attenuated. At the same time the long train of 16.7 sec. Rayleigh waves is brought out very clearly.

Figure 24 shows recordings of a teleseismic event (Gulf of California, 31.4°N, 114°W, Δ = 32.5°, origin time 07:25:36 GMT on 22 March 1969, m_b = 5.1 CGS) for the purpose of comparing the performance of the ADL and Lamont Systems at large amplitudes (in excess of 20 microns peak-to-peak). The ADL records were plotted without digital filtering. Comparison of the wave forms between the ADL and STA records shows satisfactory agreement despite the fact that the magnifications were not well matched. Again, the ADL instruments are found to be more noisy than those of the Lamont STA system; the OBS system was apparently malfunctioning.

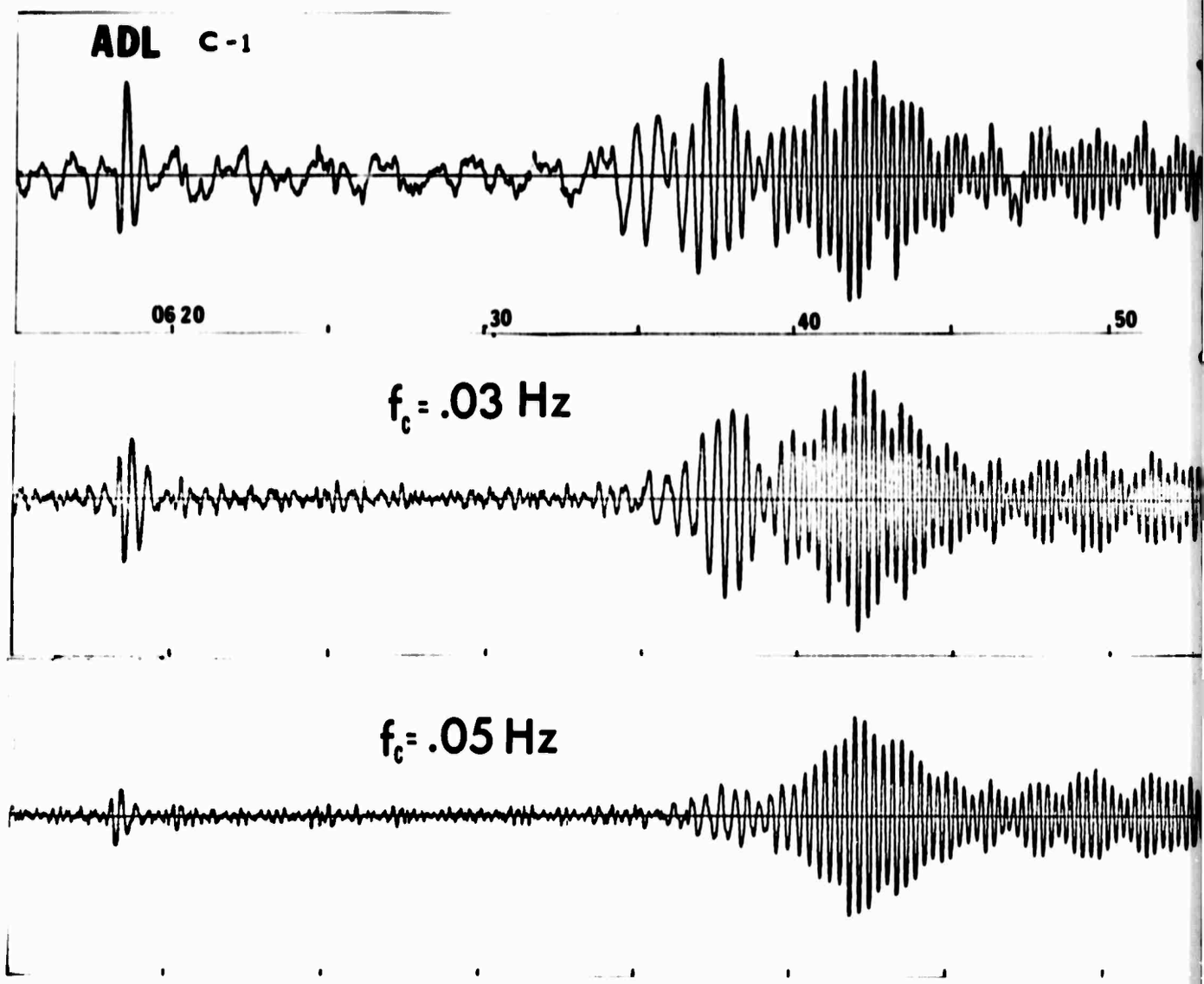

FIGURE 23 EXAMPLES OF THE EFFECT OF DIGIT
A SEISMIC RECORD; E-W COMPONENT
FIGURE 21

A.

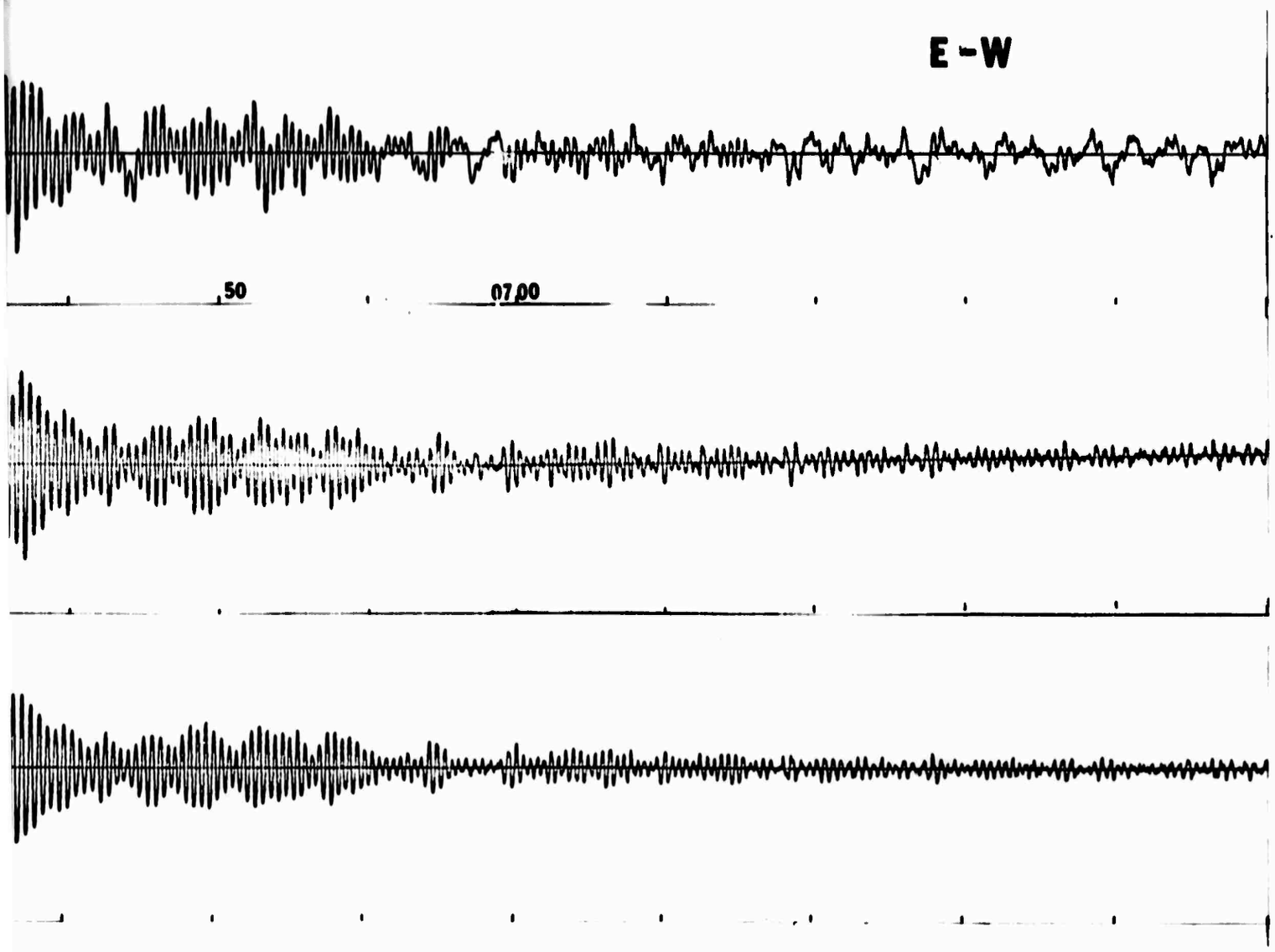

OF THE EFFECT OF DIGITAL HIGH-PASS FILTERING ON
RECORD; E-W COMPONENT OF THE SAME EVENT AS IN

B

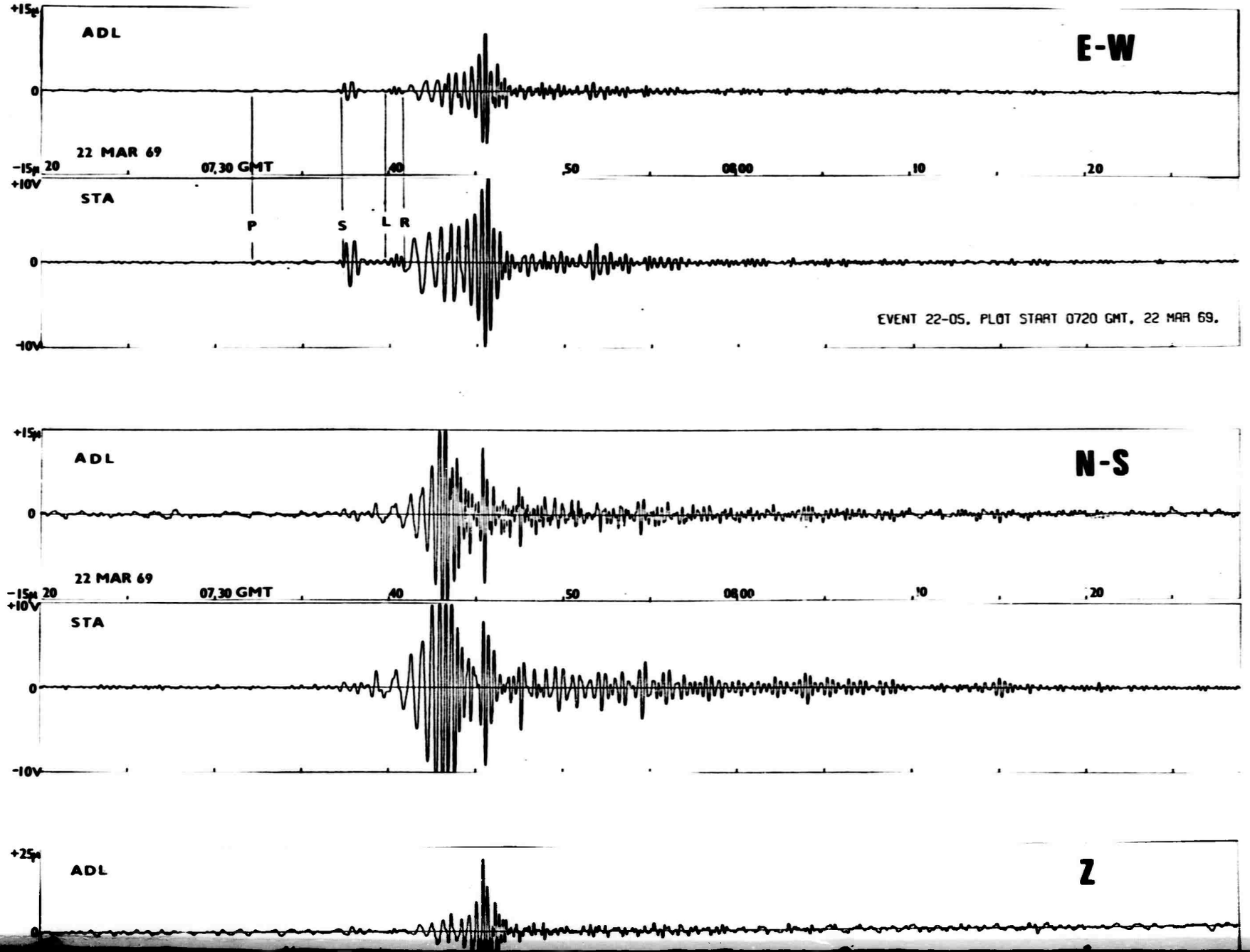
ADL
E-W
22 MAR 69
07,30 GMT
STA
P
S
L
R
EVENT 22-05, PLOT START 0720 GMT, 22 MAR 69.
ADL
N-S
22 MAR 69
07,30 GMT
STA
ADL
Z

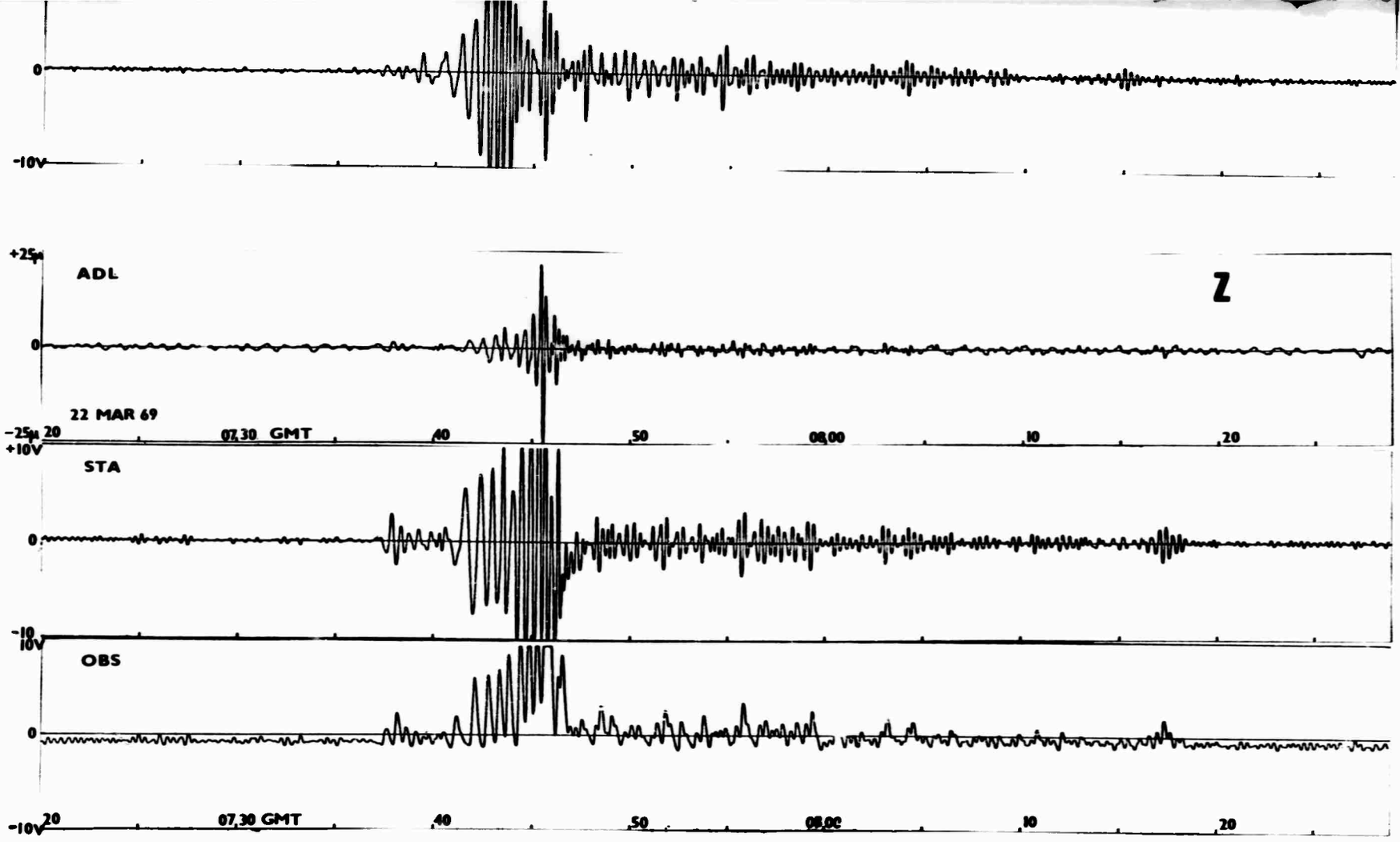

FIGURE 24 COMPARISON OF ADL AND LAMONT SYSTEMS AT LARGE SURFACE WAVE AMPLITUDES (m_b = 5.1; $\Delta = 33^{o}$; GULF OF CALIFORNIA, 31.4°N, 114°W; ORIGIN TIME 07:25:36, 22 MARCH 1969)

Figure 25 serves to illustrate the degree of response matching between pairs of instruments of the ADL system. Two horizontal (E-W) and two vertical seismograms are shown in the figure; one of the two N-S seismometers was inoperative during this period. The recordings are of the same event as that in Figure 24; however, they were digitally high-pass filtered with f_c = 0.03 Hz. Detailed examination of the records shows extremely close agreement between the seismograms both in amplitude and phase. The maximum amplitude difference between two seismometers estimated from these records appears to be less than five percent. This observation demonstrates the advantage resulting from the use of electronic feedback which makes the response of the system largely independent of the mechanical characteristics of the seismic mass and its suspension.

The last figure (Figure 26) represents a comparison between ADL and STA system at small amplitudes; all ADL records were digitally high-pass filtered with f_c = 0.03 Hz. The recordings were made during a period of high seismic activity in the Gulf of California on 21 March 1969. Three events, (labelled A, B and C) of a whole swarm of minor events are selected in Figure 26. They all occurred in the same vicinity (29.2°N, 114.4°W) and their origin times and magnitudes given in the LASA Bulletin were: Event A: 14:02:59 GMT m_b = 4.2; event B: 14:15:33 GMT m_b = 4.5; event C: 15:01:41 GMT, m_b = 4.7. Event C was subsequently reported in the CGS bulletin (PDE No. 23-69) as having magnitude m_b = 4.6.

An underground nuclear device was exploded during the same time interval at NTS, at 14:30 GMT. Its yield was reported in the press as 20 to 100 kiloton. The estimated surface wave arrival time is indicated by an arrow in Figure 26. Neither the ADL nor the Lamont long-period systems seemed to have recorded it positively

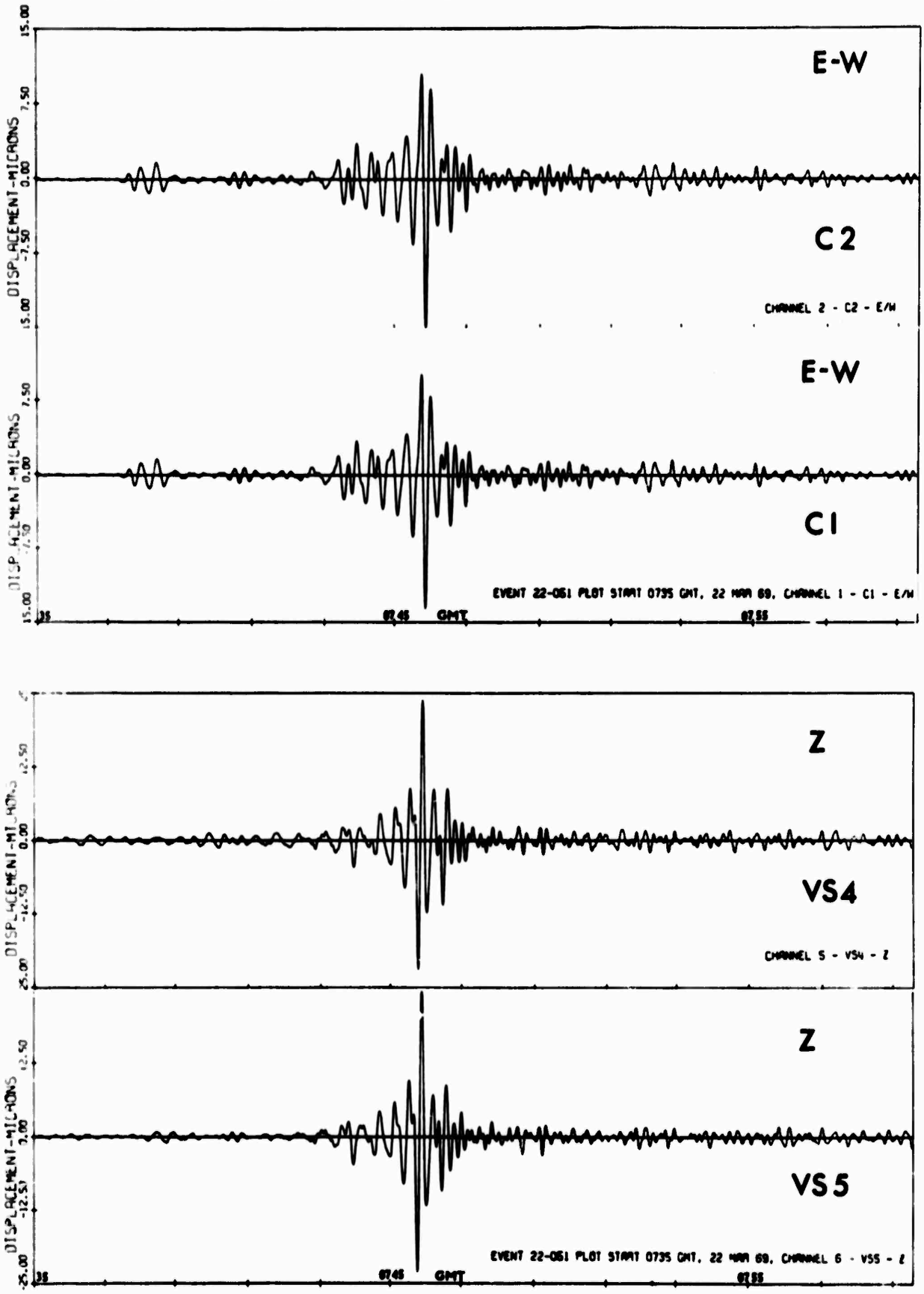

FIGURE 25 ILLUSTRATION OF THE DEGREE OF MATCHING BETWEEN TWO PAIRS OF ADL SEISMOMETERS (SAME EVENT AS IN FIGURE 24)

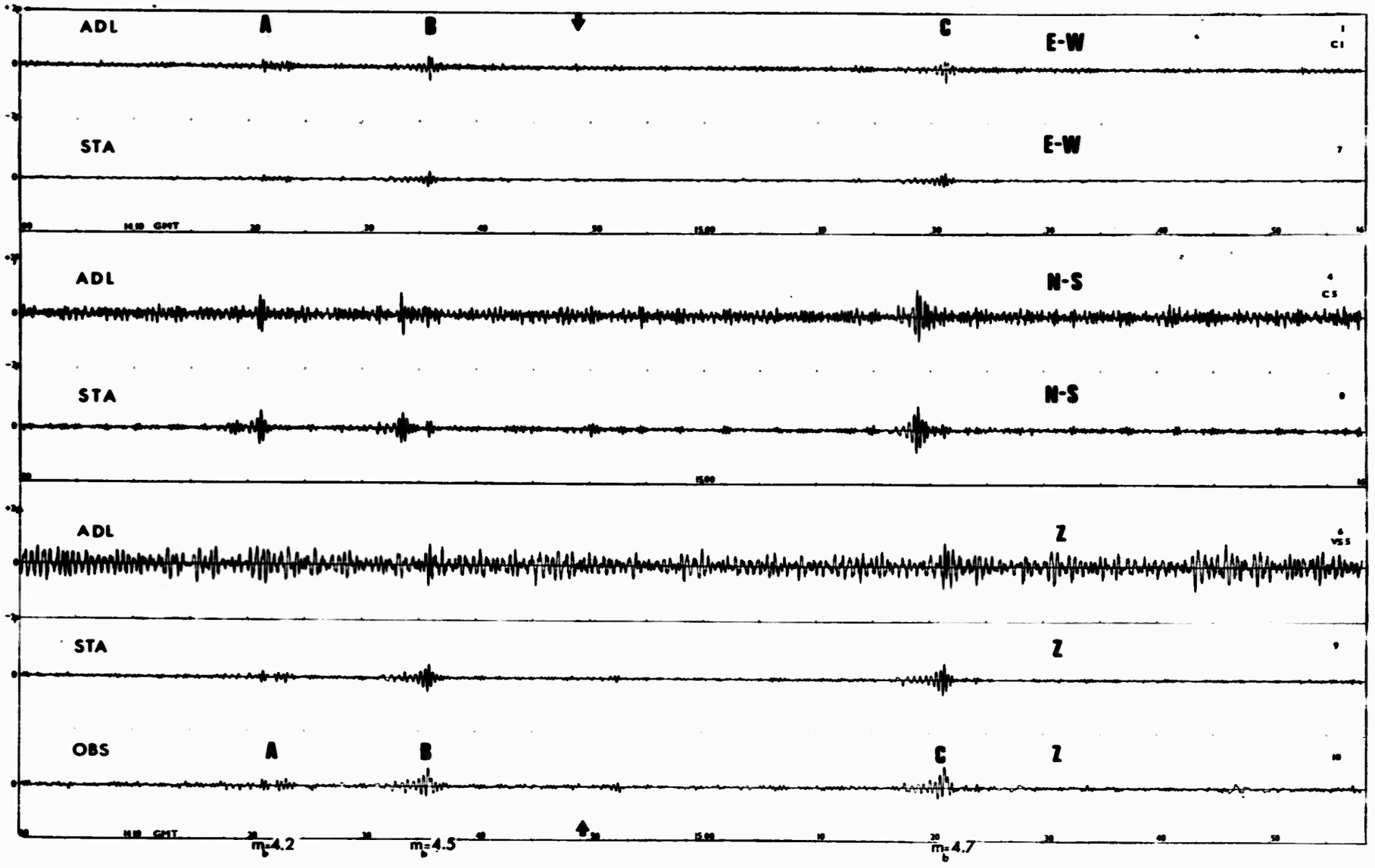

FIGURE 26 COMPARISON OF PERFORMANCE OF ADL AND LAMONT SYSTEMS AT SMALL AMPLITUDES. MAGNITUDES OF THE THREE EVENTS, OF 21 MARCH 1969, ALL ORIGINATING IN BAJA,CALIFORNIA, ARE INDICATED IN THE FIGURE. ADL RECORDS DIGITALLY FILTERED.

From the data in Figure 26 we may conclude that the horizontal seismometers of the ADL system have adequate sensitivity to detect surface waves from events of magnitude m_b = 4.2 which give rise to ground motion amplitude of approximately 0.25 microns. The vertical seismometers suffered from excessive noise which limited their detection capability to approximately m_b = 4.7. It may be further concluded that the horizontal seismometers approached the microseism-limited performance while the vertical seismometers remained limited by the instrument noise.

3. NOISE ANALYSIS

In the original feasibility study of the magnetic suspension seismometer we made an estimate of that part of the instrument noise which results from the "Brownian motion" of the seismic mass. From the equation 8 (p. III-6 of Ref. 6) we estimated for the horizontal seismometer (15 sec. natural period, 0.8 gm seismic mass, 0.025 to 0.05 Hz bandwidth and 0.7 damping ratio) r.m.s. noise displacement of approximately 12nm (120Å). For the vertical seismometer (10 sec. natural period, 9 gm seismic mass, same bandwidth and damping as above) we obtained approximately 4.3nm (43Å) for the r.m.s. noise displacement.

For the other major source of instrument noise, the photoelectric displacement sensor, we could only estimate at that time that it would be most likely of the order of 30nm (300Å) equivalent r.m.s. displacement. The remainder of the instrument noise contributed by the feedback amplifiers and the active filter was estimated to be negligible compared with the two sources of noise mentioned above. When the seismometer system was completed we wished to compare these estimates with actual measurements. Such measurements would, ideally, require the knowledge of the absolute magnitude of the ground displacement at the test site during the test and over the frequency pass band of the seismometer. Since this is practically impossible we devised various analytical methods for separating the instrument noise from the ground noise by comparison of the outputs of two or more nearly identical seismometers.

In such methods two or more of the seismometers to be tested are placed on the same pier with their input axes parallel to each other so that the seismic ground displacements

acting on them may be assumed to be identical. Their output voltages are then

$$\left.\begin{aligned} V_1 &= k_1(S+N_1)+e_1 \\ V_2 &= k_2(S+N_2)+e_2 \end{aligned}\right\} \qquad (1)$$

Here k_1, k_2, . . .denote the responsivities (volt/cm), S the seismic input displacement, N_1, N_2, . . . the noise inputs in terms of equivalent displacements, and e_1, e_2, . . . the dc offset voltages (if present). It may be safely assumed that both S and N are zero-mean quantities, and that they are completely uncorrelated. From these two assumptions it follows, respectively, that

$$\lim_{T\to\infty} \frac{1}{T} \int_0^T V_i \, dt = e_i \, , \quad \text{and} \qquad (2)$$

$$\lim_{T\to\infty} \frac{1}{T} \int_0^T V_i^2 \, dt = e_i^2 + k_i^2 \, (\overline{S^2} + \overline{N_i^2}), \qquad (3)$$

where $\overline{S^2}$ and $\overline{N_i^2}$ denote the mean square signal and noise inputs respectively. In making the integration over the time interval T the assumption is made that both S and N_i are stationary random variables in time. N_1, N_2 . . . are assumed to be mutually independent random variables.

In further discussion we shall assume that there are only two instruments being compared, which does not detract from the general validity of results. The problem is then to determine from the recorded time series of output signal values the individual contributions attributable to the signal input (in terms of $\overline{S^2}$) and to the instrument noise input ($\overline{N_i^2}$). There are basically two approaches possible toward the solution of this problem: (a) the subtractive method and, (b) the correlation method.

(a) The subtractive method is a numerical equivalent of the analog process of "bucking" the outputs of two matched seismometers and obtaining the r.m.s. values of the differential output voltage. The process of "matching" the two seismometers is replaced by the following operations:

Compute the function

$$F(b) = \frac{1}{T} \int_T (bV_1 - V_2)^2 dt \qquad (4)$$

and find the value of b which minimizes this function. Solving the integral we obtain

$$F(b) = b^2 k_1^2 \overline{N_1^2} + k_2^2 \overline{N_2^2} + (bk_1 - k_2)^2 \overline{S^2} + (be_1 - e_2) \qquad (5)$$

Assume that e_1 and e_2 are zero, or are known and have been removed from F (b). Then

$$b_{min} = \frac{k_2}{k_1} \frac{\overline{S^2}}{\overline{N_1^2} + \overline{S^2}} \qquad (6)$$

If the mean square signal $\overline{S^2}$ predominates, over the mean square noise then

$$b_{min} \to \frac{k_2}{k_1} \quad ;$$

otherwise, if the noise predominates, i.e., if $\overline{N_1^2} > \overline{S^2}$ then

$$b_{min} \to \frac{\overline{S^2}}{\overline{N^2}} \quad ;$$

b_{min} then becomes essentially the square of the signal-to-noise ratio.

In order to eliminate $\overline{S^2}$ from equation (5) so that we may solve for the $\overline{N_1^2}$ and $\overline{N_2^2}$ the appropriate value of b_m must be determined accurately; this is found to be difficult when noise predominates and signal-to-noise ratio is poor. Somewhat

better results may be obtained by defining functions G(b) or H(b) as

$$G(b) = \frac{1}{T}\int_o^T (bV_1 - b^{-1}V_2)^2\, dt,$$

$$H(b) = \frac{1}{T}\int_o^T [(1+b)V_1 - (1-b)V_2]^2\, dt.$$

However, the improvement is only marginal and the subtractive method was found in general impractical.

(b) The correlation method makes use of the assumption that the input signals S, N_1 and N_2 are statistically independent random variables. Consequently, their cross products in the function

$$M_{12} = \frac{1}{T}\int_o^T V_1V_2\, dt \qquad (7)$$

have zero mean values, as well as S_1, N_1 and N_2 themselves; hence

$$M_{12} = k_1k_2\overline{S^2} + e_1e_2$$

since from equation (2) $e_1 = \overline{V_1}$ and $e_2 = \overline{V_2}$ we obtain the mean square seismic displacement

$$\overline{S^2} = \frac{M_{12} - \overline{V_1}\,\overline{V_2}}{k_1k_2} \qquad (8)$$

Furthermore, from equation (3) and equation (2) we obtain for the sum of the mean square values of the seismic and noise displacements

$$\left.\begin{aligned} \overline{S^2} + \overline{N_1^2} &= \frac{\overline{V_1^2} - (\overline{V_1})^2}{k_1^2} \\ \text{and} \qquad \overline{S^2} + \overline{N_2^2} &= \frac{\overline{V_2^2} - (\overline{V_2})^2}{k_2^2} \end{aligned}\right\} \qquad (9)$$

Thus the $\overline{S^2}$ and $\overline{N_1^2}$, $\overline{N_2^2}$ can be individually determined.

In performing the numerical analysis of actual test results the integrals defining the functions F, M_{12} etc. become summations with small increments of variables over finite time intervals. The test data exist in a form of time series of numerical values of all instrument output voltages since they were recorded in this manner by the incremental digital recorder. The time increments were fixed by the sampling rate of the multiplexer which was, typically, 3.3 sec. for each of the ten recorded channels.

The selection of a data sample suitable for analysis and the choice of the proper integration time deserves some attention. The data should be selected from a time interval during which no seismic events occurred and the microseismic activity was low and uniform (stationary). This consideration puts a limit on the maximum length of integration interval. If the integration time is chosen too long errors may arise from non-stationarity of the time series, small seismic events may become included in the data and drifts in the d.c. offset may creep in. On the other hand, the use of a short integration time leads to large statistical errors. The variance of a mean square value is approximately $(T\,\Delta f)^{-2}$ where T is the integration time and Δf is the bandwidth. For our seismometers $\Delta f \approx 0.025$ Hz. If T is chosen to be one-half of an hour (1800 sec.)--which is as long as practically feasible--the variance is $(45)^{-2} \approx 0.15$, or 15 percent, which is acceptable.

For example, we selected data from a recording made on 26 February 1969 between hours 0330 and 1300 GMT for correlation analysis of two horizontal seismometers C-1 and C-2. Integration time of 1800 seconds was chosen and twenty sums of the quantities $\overline{V_1^2}$, $\overline{V_2^2}$ and $\overline{V_1V_2}$ were computed. Mean values of these twenty sums were respectively 33.2 ± 5.0, 45.5 ± 3.6 and -2.59, all in 10^{-6} volt ^{2}. The small value of the $\overline{V_1V_2}$ product indicates a small degree of correlation between the two seismometers;

consequently their output must be largely due to instrument noise. Performing the calculations outlined above we obtained for the r.m.s. values of the noise displacement 0.15μm, and 0.14μm, respectively for C-1 and C-2 instruments. Some of this excess noise is due to the quantization noise in the A/D converter; since the sampling quantum was 2.5 mv, the r.m.s. sampling noise was approximately 0.7 mv or approximately 0.02μm r.m.s. equivalent displacement noise.

By comparison we analyzed a block of data from 0730 to 0800 GMT of 25 February 1969 which included an earthquake of magnitude 5.7 in Honduras. The mean-square voltages and cross product values were for the two seismometers: $\overline{V_2^2}$ = 123.74, $\overline{V_2^2}$ = 164.09 and $\overline{V_1 V_2}$ = 87.31, all in 10^{-6} volt^2. The calibration of the two instruments were k_1 = 384V/cm and k_2 = 484V/cm. Using these values we obtain

$$\overline{N_1^2} = 123.74 - 87.31\ (384/484) = 54.4 \times 10^{-6} V^2$$

and

$$\overline{N_2^2} = 164.09 - 87.31\ (484/384) = 54.0 \times 10^{-6} V^2.$$

This corresponds to 7.3 mv r.m.s. noise voltage or approximately 0.16μm r.m.s. equivalent noise displacement, in agreement with the previous figures.

Similarly, we analyzed the outputs of the two vertical seismometers VS-4 and VS-5 for the same time period in 26 February 1969. The mean square values of $\overline{V_4^2}$ and $\overline{V_5^2}$ were 358 $\pm$ 77 and 87 $\pm$ 20 x 10^{-4} volt^2; with responsivities k_4 = 2120V/cm and k_5 = 2060V/cm (including 100X post-amplification) this corresponds to equivalent r.m.s. noise displacements of 0.89 and 0.45μm. Obviously, the vertical seismometers generated instrument noise an order of magnitude greater (in r.m.s. values) than the horizontal instruments.

Since the vertical seismometers employ optical detectors essentially identical with those used in the horizontal seismometers and their Brownian motion noise must be smaller on account of their greater seismic mass, we must conclude that the excess noise results from other causes such as smaller transducer sensitivity, higher post-amplifier gain, air convection currents in the instrument case and fluctuations in the period control current supply. Even though we were unable to resolve exactly the relative contributions of these sources of noise we have reasons to believe that the effect of any or all of them could be substantially reduced and the performance of the vertical seismometer improved to be at least as good as that of the horizontal ones. The steps to be made toward the reduction of instrument noise should include: evacuation of the seismometer case; increase of transducer responsivity; individual selection of photocells for low noise; selection of low-noise amplifiers. These steps are all practically feasible and within the state of the art.

IV. CONCLUSIONS

- Practical feasibility of highly compact long-period, feedback-controlled seismometers utilizing a novel magnetic suspension was demonstrated.

- An experimental system comprising two E-W, two N-S and two vertical component seismometers, electronic feedback controls, band-pass filters and a multi-channel digital recorder was constructed and tested at the Ogdensburg, New Jersey deep mine seismological station alongside Lamont-Doherty Observatory's systems.

- Surface waves from earthquakes of body-wave magnitudes $m_b \lesssim 5$ at teleseismic distances ($\Delta \approx 30°$ to $140°$) were consistently recorded. The smallest detectable magnitude (from the Gulf of California region) was $m_b \doteq 4.2$ with the horizontal seismometers and $m_b \doteq 4.7$ with the vertical seismometers.

- The performance of the seismometers was limited by their instrument noise. Analysis of the noise data indicated areas in which considerable improvement can be achieved.

V. ACKNOWLEDGMENTS

I wish to thank Dr. J. E. Oliver, Director of the Seismology Division, Lamont-Doherty Geological Observatory for making available to us the facilities at the Sterling Forest and Ogdensburg Seismological Stations for final tests. John Savino gave us valuable help in coordinating the tests between Lamont-Doherty Observatory, New Jersey Zinc Co. and Arthur D. Little, Inc. Merrill Conner and George Hade of the observatory's operating staff have our thanks for the generous assistance in the installation and operation of the equipment during the tests in the mine. We are also indebted to Mr. R. L. Wood, Manager and R. W. Metsger, Chief Geologist of the Sterling Mine of the New Jersey Zinc Co. at Ogdensburg, New Jersey for every assistance extended to us during our stay at the mine.

VI. REFERENCES

1. Evernden, J. F., Identification of Earthquakes and Explosions by use of Teleseismic Data. J. Geophys. Res., 74, 3828 - 3856, (1969).
2. Brune, J. N., A. Espinosa and J. Oliver, Relative Excitation of Surface Waves by Earthquakes and Underground Explosions in the California - Nevada Region, J. Geophys. Res., 68, 3501 - 3512, (1963).
3. Pomeroy, P. W., J. Savino, G. Hade and R. Chandar, Preliminary Results from High-Gain Wide-Band Long-Period Electromagnetic Seismograph System. J. Geophys Res. 74, 3295 - 3298, (1969).
4. Simon, I., A. G. Emslie, P. F. Strong and R. K. McConnell, Jr., Sensitive Tiltmeter utilizing Diamagnetic Suspension, Rev. Sci. Instr., 39, 1666 - 1671, (1968).
5. Haubrich, R. A. and Keith McCamy, Microseisms: Coastal and Pelagic Sources, Rev. of Geophysics, 7, 539 - 571, (1967).
6. Development of a Three-Axis Long-Period Seismograph, Annual report, Arthur D. Little, Inc., AFOSR Contract No. F44620-67-C-0107, (31 May 1968).
7. Handbook of Operational Amplifier Active RC Networks, pp. 80 - 83, Burr-Brown Research Corp., Tucson, Arizona, (1966).
8. Sutton, G. H. and G. V. Latham, Analysis of a Feedback Controlled Seismometer, J. Geophys. Res., 69, 3865, (1964).

BLANK PAGE

UNCLASSIFIED
Security Classification

DOCUMENT CONTROL DATA - R & D

(Security classification of title, body of abstract and indexing annotation must be entered when the overall report is classified)

1. ORIGINATING ACTIVITY (Corporate author)
Arthur D. Little, Inc.
25 Acorn Park
Cambridge, Massachusetts 02140

2a. REPORT SECURITY CLASSIFICATION
UNCLASSIFIED

2b. GROUP

3. REPORT TITLE
Development of a Three-Axis Long-Period Seismograph

4. DESCRIPTIVE NOTES (Type of report and inclusive dates)
Scientific ..... Interim

5. AUTHOR(S) (First name, middle initial, last name)
Ivan Simon

6. REPORT DATE
16 February 1970

7a. TOTAL NO. OF PAGES
68

7b. NO. OF REFS
8

8a. CONTRACT OR GRANT NO.
F44620-67-C-0107

b. PROJECT NO
8652

c. 62701D

d.

9a. ORIGINATOR'S REPORT NUMBER(S)

9b. OTHER REPORT NO(S) (Any other numbers that may be assigned this report)
AFOSR 70-0526 TR

10. DISTRIBUTION STATEMENT
1. This document has been approved for public release and sale; its distribution is unlimited.

11. SUPPLEMENTARY NOTES
TECH, OTHER

12. SPONSORING MILITARY ACTIVITY
AF Office of Scientific Research (SRPG)
1400 Wilson Boulevard
Arlington, VA 22209

13. ABSTRACT

Three-axis, long-period, compact (borehole) seismometer system utilizing feedback-controlled seismic transducers based on magnetic suspension principle was developed, constructed and tested. The system includes digital tape recording and data processing. The overall system response is flat to 3db over a pass band from .02 to .07 Hz and the dynamic range is 60db. Results of tests show that surface waves from teleseismic events of $m_b \leq 5$ are consistently recorded. Horizontal components of surface waves from earthquakes as small as $m_b \approx 4.2$ in the Gulf of California region have been observed at the Ogdensburg, New Jersey test site.

DD FORM 1 NOV 68 1473

UNCLASSIFIED
Security Classification

14 KEY WORDS	LINK A		LINK B		LINK C	
	ROLE	WT	ROLE	WT	ROLE	WT
Long-period seismometers Borehole seismometer Surface wave detection						

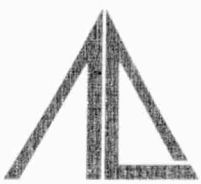

Arthur D. Little, Inc.

CAMBRIDGE,
MASSACHUSETTS

CHICAGO
SAN FRANCISCO
SANTA MONICA
WASHINGTON
ATHENS
BRUSSELS
LONDON
MEXICO CITY
PARIS
RIO DE JANEIRO
TORONTO
ZURICH